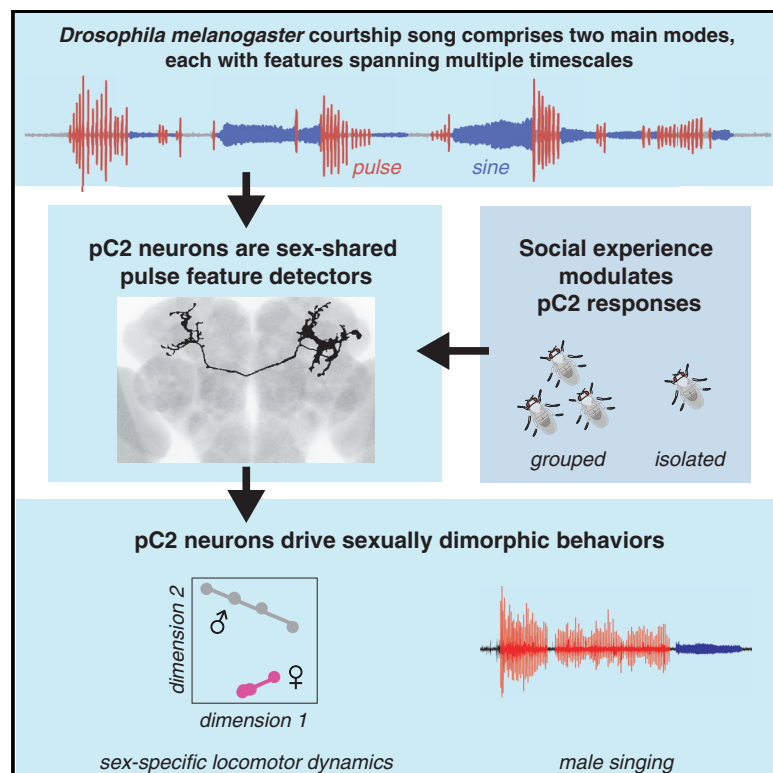


Shared Song Detector Neurons in *Drosophila* Male and Female Brains Drive Sex-Specific Behaviors

Graphical Abstract



Authors

David Deutsch, Jan Clemens,
Stephan Y. Thibierge, Georgia Guan,
Mala Murthy

Correspondence

mmurthy@princeton.edu

In Brief

Communication signals can evoke sex-specific responses. Using quantitative behavior, calcium imaging, and neural manipulations, Deutsch et al. find that sex-shared neurons in *D. melanogaster* are tuned for the multiple spectrotemporal features that define courtship song. These neurons drive sex-specific behaviors, linking feature detection to action.

Highlights

- *D. melanogaster* males and females are selective for multiple song features
- These song features drive divergent responses in males and females
- pC2 neurons serve as shared song feature detectors in males and females
- pC2 neurons are critical for sex-specific responses to courtship song



Shared Song Detector Neurons in *Drosophila* Male and Female Brains Drive Sex-Specific Behaviors

David Deutsch,^{1,4} Jan Clemens,^{1,2,4} Stephan Y. Thibierge,^{1,3} Georgia Guan,¹ and Mala Murthy^{1,3,5,*}

¹Princeton Neuroscience Institute, Princeton University, Princeton, NJ 08540, USA

²European Neuroscience Institute Göttingen – A Joint Initiative of the University Medical Center Göttingen and the Max-Planck Society, Grisebachstrasse 5, Göttingen 37077, Germany

³Bezos Center for Neural Circuit Dynamics, Princeton Neuroscience Institute, Princeton University, Princeton NJ 08540, USA

⁴These authors contributed equally

⁵Lead Contact

*Correspondence: mmurthy@princeton.edu

<https://doi.org/10.1016/j.cub.2019.08.008>

SUMMARY

Males and females often produce distinct responses to the same sensory stimuli. How such differences arise—at the level of sensory processing or in the circuits that generate behavior—remains largely unresolved across sensory modalities. We address this issue in the acoustic communication system of *Drosophila*. During courtship, males generate time-varying songs, and each sex responds with specific behaviors. We characterize male and female behavioral tuning for all aspects of song and show that feature tuning is similar between sexes, suggesting sex-shared song detectors drive divergent behaviors. We then identify higher-order neurons in the *Drosophila* brain, called pC2, that are tuned for multiple temporal aspects of one mode of the male's song and drive sex-specific behaviors. We thus uncover neurons that are specifically tuned to an acoustic communication signal and that reside at the sensory-motor interface, flexibly linking auditory perception with sex-specific behavioral responses.

INTRODUCTION

Across animals, males and females produce distinct, dimorphic behaviors in response to common sensory stimuli (e.g., pheromones, visual cues, or acoustic signals), and these differences are critical for social and reproductive behaviors [1, 2]. It remains open as to how sex-specific behaviors to common sensory signals emerge along sensorimotor pathways. It could be that males and females process sensory information differently, leading to different behavioral outcomes, or that males and females process sensory information identically but drive different behaviors downstream of common detectors.

This issue has been most heavily investigated for pheromone processing. In *Drosophila*, the male pheromone cVA induces either aggression in males [3] or receptivity in females [4, 5]. The pheromone is detected by shared circuits in males and

females, and the sensory information [6] is then routed to sex-specific higher-order olfactory neurons [7, 8] that likely exert different effects on behavior. In the mouse, the male pheromone ESP1 triggers lordosis in females but has no effect on male behavior. This pheromone activates V2Rp5 sensory neurons in both sexes but, analogous to cVA processing in flies, these neurons exhibit sex-specific projection patterns in the hypothalamus that drive sex-specific behavioral responses [9, 10]. For pheromone processing then, the rule appears to be that early olfactory processing is largely shared between the sexes and then common percepts are routed to separate higher-order neurons or circuits for control of differential behaviors. But does this rule apply for other modalities or for stimuli that can be defined by multiple temporal or spatial scales (e.g., visual objects or complex sounds)? For such stimuli, selectivity typically emerges in higher-order neurons [11–13], and we do not yet know if such neurons are shared between males and females and therefore whether dimorphic responses emerge in downstream circuits.

Here, we investigate this issue in the auditory system of *Drosophila*. During courtship, males chase females and produce a species-specific song that is comprised of two major modes—pulse song consists of trains of brief pulses and sine song consists of a sustained harmonic oscillation [14]. In contrast with males, females are silent but arbitrate mating decisions. Males use visual feedback cues from the female to determine which song mode (sine or pulse) to produce over time [15–17]; this gives rise to the variable structure of song bouts (Figure 1A). Receptive females slow in response to song [15, 18–24], while playback of courtship song to males in the presence of other flies can induce them to increase their walking speed [21, 24, 25] and to display courtship-like behaviors [26–29]. Here, we investigate whether males and females share common sensory detection strategies for their courtship song and how divergent behaviors arise.

Each major mode of *Drosophila* courtship song, sine or pulse, contains patterns on multiple temporal scales [14, 30] (Figure 1A)—neurons that represent either the pulse or sine mode should in theory bind all of the temporal features of each mode, similar to object detectors in other systems [11, 31–33], and their tuning should match behavioral tuning. Historically, behaviorally relevant song features have been defined based



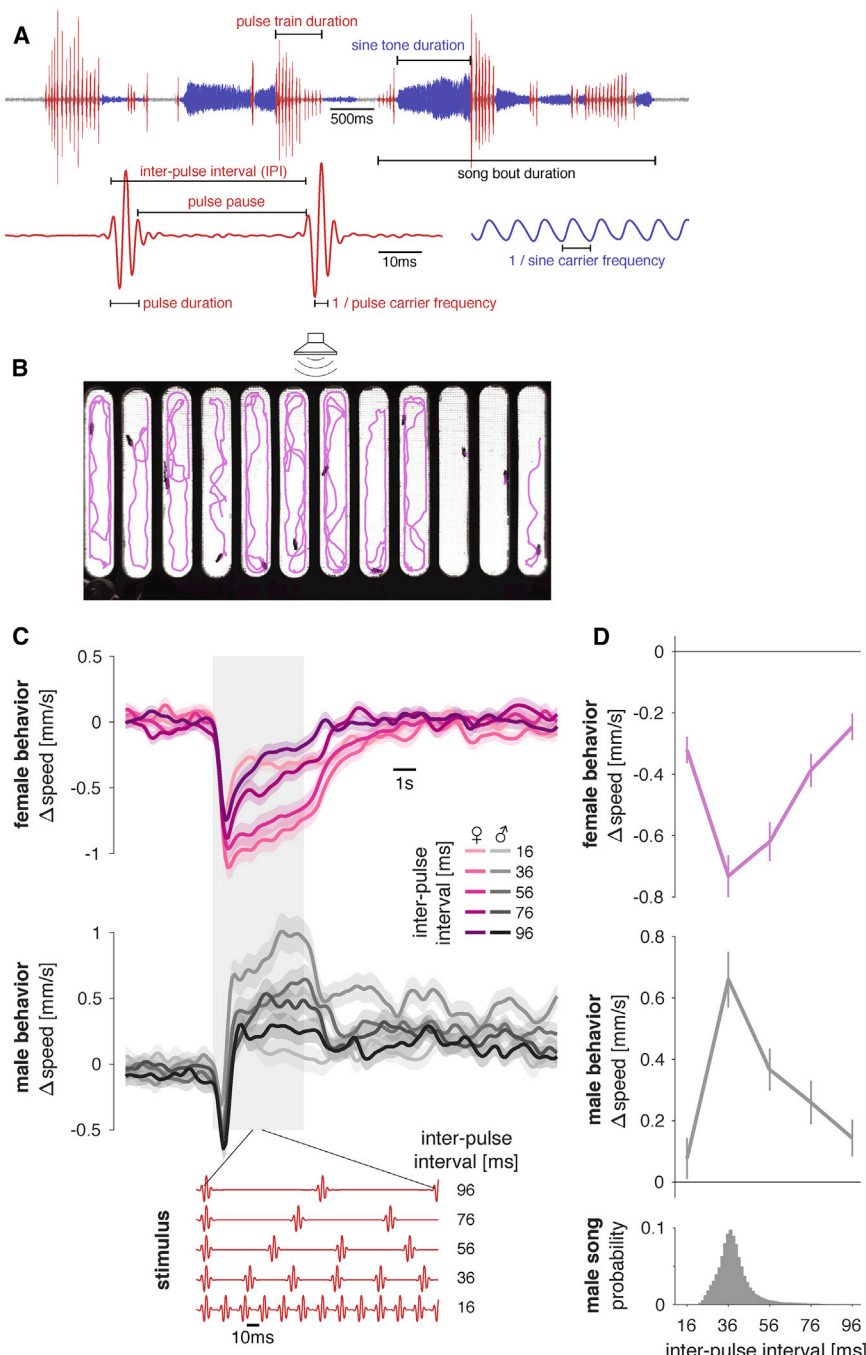


Figure 1. FLyTRAP Assay for Comparing Locomotor Tuning for Courtship Song Stimuli in Males and Females

(A) *Drosophila melanogaster* produces song in bouts that can consist of two modes: sine song corresponds to a weakly amplitude modulated oscillation with a species-specific carrier frequency (~150 Hz) and pulse song corresponds to trains of Gabor-like wavelets each with a carrier frequency between 220 and 450 Hz and a duration between 6 and 12 ms. These pulses are produced at an inter-pulse interval (IPI) of 30–45 ms.

(B) FLyTRAP consists of a behavioral chamber that is placed in front of a speaker through which sound is presented. Fly movement is tracked using a camera. Shown is a single video frame of females in the assay with fly tracks for the preceding 20 s overlaid in magenta. See Video S1.

(C) Locomotor responses of females (magenta) and males (gray) for pulse trains with different IPIs (see legend). The gray shaded box indicates the duration of the sound stimulus. Red traces at the bottom of the plot show short snippets of five of the stimuli presented in this experiment. The baseline speed was subtracted before trial averaging.

(D) Speed tuning curves for different IPIs in females (magenta) and males (gray) are obtained by averaging the speed traces in the 6 s following stimulus onset. The histogram at bottom shows the IPI distribution found in male song (data from 47 males of NM91 wild-type strain totaling 82,643 pulses).

Lines and shaded areas or error bars in (C) and (D) correspond to the mean \pm SEM across 112 male and 112 female flies. All Δ speed values from the wild-type strain NM91. See also Figure S1, Video S1, and Table S1.

on the parameters of the species' own song. However, there is now ample evidence that the preferred song can diverge from the conspecific song [34–36]—for instance, females may prefer exaggerated song features [37, 38] or respond to signal parameters not normally produced by their male conspecifics [39]. It is therefore important to define song modes by the acoustic tuning of specific behavioral outputs. This has been done for other insects (e.g., [40, 41]) but never for flies in a systematic way that also permits a direct comparison between sexes.

To that end, we developed a behavioral assay for assessing dynamic changes in walking speed in response to sound playback in both sexes, and we then measured locomotor tuning for all features of either pulse or sine song. We found that males and females have similar tuning but different behavioral responses and that they are tuned for every major feature of the song. We then identified a set of sexually dimorphic neurons, termed pC2 [42, 43, 44], that serve as shared pulse song detectors in both sexes: the tuning of pC2 neurons is matched to behavioral tuning for pulse song across a wide range of temporal scales. We find that optogenetic activation of pC2 is sufficient to drive sex-specific behaviors and that silencing pC2 neurons biases males to production of sine song. pC2 is therefore important both for pulse song processing and pulse song generation. Finally, we show that early social experience changes both the tuning of pC2 neurons and behavior. Our results indicate that the fly brain contains common pulse song

detectors in males and females, which control sex-specific behavioral responses to song via downstream circuits.

RESULTS

Comprehensive Characterization of Behavioral Tuning for Courtship Song Features

We designed a single-fly playback assay in which individual males or females receive acoustic stimuli in the absence of any confounding social interactions, and we implemented an automated tracker to analyze changes in locomotion relative to acoustic playback (Figure 1B; Video S1). The assay (which we refer to as FLyTRAP [fly locomotor tracking and acoustic playback]) monitors dynamic changes in walking speed, which provides a readout that can be directly compared between both males and females, as opposed to slower readouts of sex-specific behaviors such as the female time to copulation [43, 45] or male-male chaining [27, 28]. Because of the high-throughput nature of our assay combined with automated tracking, we can easily test a large number of flies and song parameters, including those only rarely produced by conspecifics but to which animals might be sensitive. Using FLyTRAP, we systematically compared male and female locomotor tuning to 82 acoustic stimuli that span the features and timescales present in courtship song (see Table S1). Typically, each stimulus was presented 23 times to 120 females and 120 males, generating >2,500 responses per stimulus and sex (see STAR Methods).

We first examined behavioral tuning for inter-pulse interval (IPI) using the wild-type strain NM91 (Figure 1A), whose acoustic response during courtship was previously characterized [17]. Observed changes in speed were stimulus locked, sex specific, and tuned to IPI (Figure 1C). Varying stimulus intensity had minimal effect on pulse song responses (Figures S1A and S1B). While females slowed down to pulse trains, males exhibited transient slowing at pulse train onset followed by a long-lasting acceleration. The transient component of the locomotor response was present for all stimuli (Figures S2A–S2C) and may correspond to an unspecific startle response to sound onset [46]. The transient was also present in females but masked by the stimulus-dependent slowing that followed (Figure 1C). Due to the brevity of the transient response, the integral change in speed following stimulus onset reflects mostly the speed during the sustained phase (Figures S1C–S1D). For simplicity, we therefore used the full integral as an overall measure of behavioral tuning. We found that, in FLyTRAP, female IPI tuning is a band-pass-filter matched to the statistics of male song (Figure 1D): the mode of the distribution of *Drosophila melanogaster* IPIs is centered between 30 and 50 ms, and females decrease their speed most for the same IPI range. Males produced a similar band-pass-tuning curve peaked at the same IPI range, but their locomotor response was opposite in sign (males accelerated, females decelerated). This is consistent with the results of other assays (male-female copulation rates or male-male chaining) that have found band-pass tuning for IPI in both sexes [21, 27, 45, 47] and a sex-specific sign of locomotor responses [21, 24].

We found the behavioral tuning for IPI in seven additional wild-type strains to still be sex specific but different from strain NM91 (Figure S1E). For the subsequent analyses of locomotor tuning in

FLyTRAP, we chose the NM91 strain as (1) it produced responses to song that were similar to the genetic background used for calcium imaging experiments (Figures S1F–S1I), and (2) it produced song responses that were consistent with those found using other assays [21, 24, 28, 29]—for example, showing slowing to pulse song in females versus acceleration to pulse song in males.

We next systematically varied parameters that characterize pulse song to cover (and extend beyond) the distribution of each parameter within *D. melanogaster* male song (see Figure S2). We examined behavioral tuning in both sexes for parameters that varied on timescales of milliseconds (carrier frequency, pulse duration, and IPI) to seconds (pulse train duration) (Figure 1A). We found that male and female tuning curves are of opposite sign but similar shape for all pulse song features tested across timescales (Figures 2A, 2B, and S2A–S2F), and that the behavioral tuning for pulse parameters often overlapped the distribution found in natural song (Figure 2C). While the behavioral tuning curves for all pulse song features on short timescales are band pass with a well-defined peak, we found that tuning for pulse train duration was monotonic: both females and males increase their locomotor response with increasing pulse train duration up to 4 s (Figures 2A and 2B). During natural courtship, pulse trains longer than 4 s are rarely produced [15]—these stimuli thus correspond to “supernormal” stimuli, which drive strong responses probably due to integration over long timescales [48]. Males also produce two distinct types of pulses [17]—we find that, while females appear to be broadly tuned for both types of pulses in the FLyTRAP assay, males respond preferentially to higher-frequency pulses (Figures 2A and 2B). Finally, we found that both males and females are more selective for the pulse duration versus the pulse pause, the two components of the IPI (Figures S2D–S2F)—this is in contrast to other insects that produce and process song pulses (e.g. crickets, grasshoppers, katydids) and that are preferentially tuned to pulse pause, pulse period, or pulse train duty cycle [49, 50].

We next tested locomotor tuning for the parameters that characterize sine stimuli—carrier frequency and the duration of sine trains (Figure 1A). Both males and females slow for sine tones of different frequencies, with very low and very high frequencies eliciting the strongest responses (Figures 2A, 2B, and S2A–S2C). Notably, the frequencies inducing the strongest slowing are not typically produced by males (Figure 2C). As for sine train duration tuning, we observed sustained responses that increased with duration and saturated only weakly, possibly because of the weak response magnitude.

Pulse and sine song usually co-occur within a single bout, but it is not known why males produce two different modes (although females respond to both during natural courtship [15, 17]). One possibility is that one mode exerts a priming effect on the other [51]. We presented sequences in which a pulse train was followed by a sine tone or vice versa and compared the responses for these sequences to the responses to an individual pulse train or sine tone (Figure S2G). The responses are well explained by a linear combination of the responses to individual sine or pulse trains. Deviations from linearity occur due to sound onset responses, but otherwise responses do not strongly depend on the order of presentation

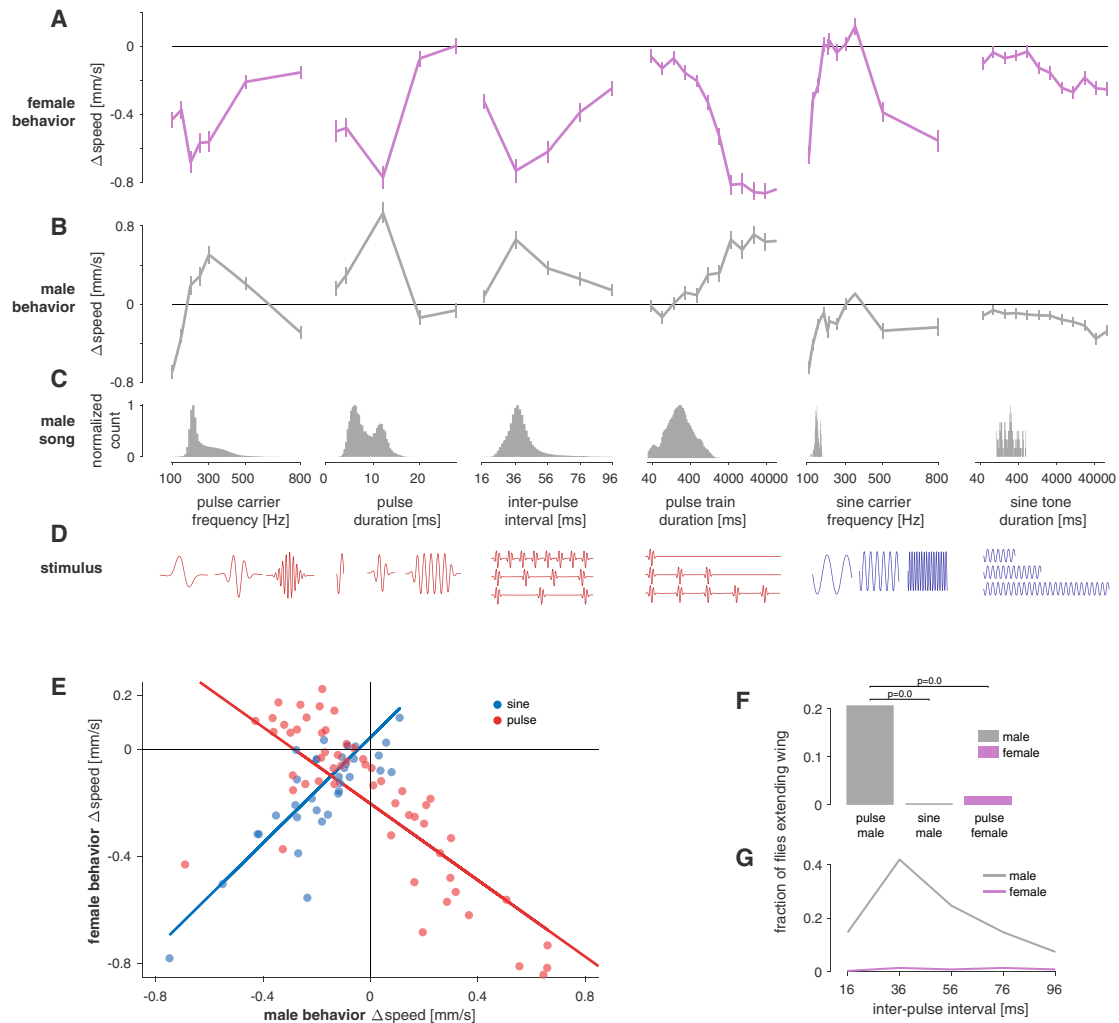


Figure 2. Responses to Song Playback Are Sex Specific and Tuned for Multiple Features of Pulse and Sine Song

(A and B) Locomotor tuning curves for females (A, magenta) and males (B, gray) for 6 different features of pulse and sine song. Lines and error bars correspond to the mean \pm SEM across flies (see Table S1 for a description of all stimuli and n files).

(C) Distribution of the six different song features tested in (A) and (B) in the natural courtship song of *Drosophila melanogaster* males (data from 47 males of NM91 wild-type strain totaling 82,643 pulses and 51 min of sine song from 5,269 song bouts). Histograms are normalized to a maximum of 1.0.

(D) Pictograms (not to scale) illustrating each song feature examined in (A)–(C). Pulse and sine song features are marked red and blue, respectively.

(E) Changes in speed for males and females for all pulse (red) and sine (blue) stimuli tested (data are from A, B, and Figure S2). Each dot is the average behavioral response for one pulse or sine stimulus. Responses to sine stimuli are strongly and positively correlated between sexes ($r = 0.89$, $p = 6 \times 10^{-8}$). Pulse responses are also strongly but negatively correlated ($r = -0.63$, $p = 5 \times 10^{-10}$). Blue and red lines correspond to linear fits to the responses to sine and pulse song, respectively.

(F) Fraction of trials for which male and female flies extended their wings during the playback of pulse song (five different IPIs as in Figures 1C and 1D) and sine song (150 Hz, quantified only for males). Solitary males (gray) frequently extend their wings in response to pulse but not to sine song. Solitary females (magenta) do not extend wings for pulse song. See also Video S2. p values were obtained from a two-sided chi-square test.

(G) Fraction of trials that evoke wing extension in males (gray) and females (magenta) as a function of IPI. In males, wing extension and locomotor behavior (Figure 1D) exhibit strikingly similar tuning with a peak at the conspecific IPI. Females almost never extend their wing for any IPI.

All behavioral data are from the wild-type strain NM91. All correlation values are Spearman's rank correlation. See also Figures S1 and S2, Video S2, and Table S1.

in a bout (see also [52]). This suggests that these stimuli are processed in independent pathways.

To summarize, we compared behavioral responses in males and females for all features that define the courtship song. Male and female speed changes were strongly correlated for both song modes, but the sign of the correlation was negative for pulse stimuli and positive for sine stimuli (Figure 2E). The

opposite sign of the correlations along with the independence of responses to sine and pulse stimuli (Figure S2G) indicates that sine and pulse song are processed by different circuits. The large magnitude of the correlations implies that feature tuning of the behavioral responses is similar between sexes and suggests that detector neurons for each song mode are shared between sexes.

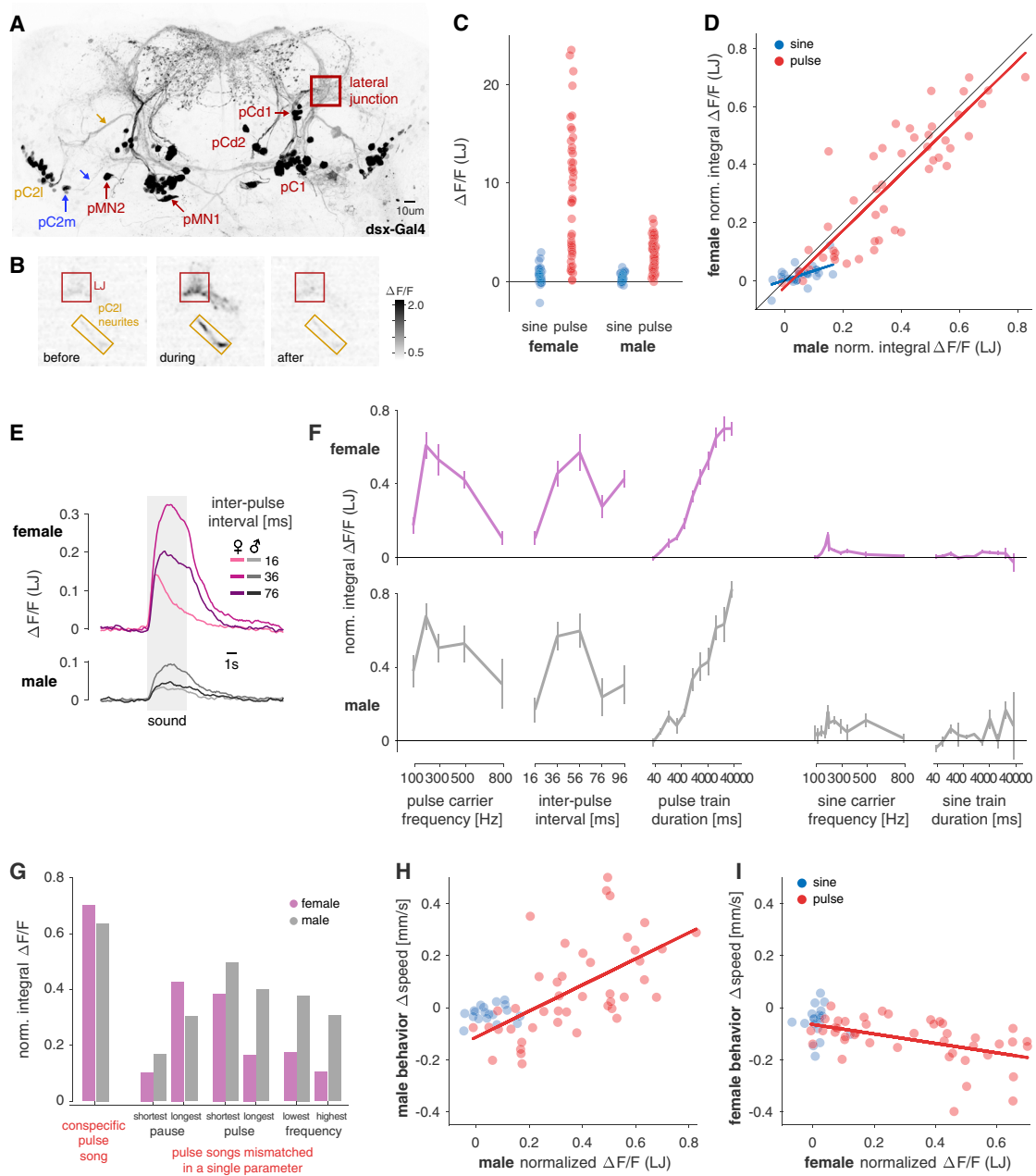


Figure 3. Neuronal Tuning of Dsx+ Neurons in the LJ Matches Behavioral Tuning for Pulse Stimuli in Males and Females

(A) Anatomy of Dsx+ neurons in the female brain. Max z-projection of a confocal stack of a fly brain in which all Dsx+ are labeled with GFP. 5/8 cell types (pC1, pC2l [yellow], pC2m [blue], pMN1, pMN2) project to the LJ, while 3 cell types (pCd1, pCd2, aDN) do not. Yellow and blue arrows point to the neurites that connect pC2l and pC2m to the LJ. See also Figures S4B and S4C.

(B) Grayscale image (see color bar) of calcium responses ($\Delta F/F$) to a pulse train (IPI 36 ms) in a region of interest (ROI) centered around the LJ (red) and the pC2l neurites (yellow) in a female. Shown are snapshots of the recording at three different time points relative to stimulus onset—before ($T = -10$ s), during ($T = 1.2$ s), and after ($T = 20$ s) the stimulus. Flies express GCaMP6m in all Dsx+ cells. Conspecific pulse song elicits strong increases in fluorescence in the LJ and the pC2l neurites.

(C) LJ responses to sine (blue) and pulses (red) stimuli in females (left) and males (right). Individual dots correspond to average integral $\Delta F/F$ responses (across 3–12 flies per stimulus) for individual pulse and sine stimuli. Many pulse stimuli evoke much stronger responses than the most effective sine stimulus ($p = 8 \times 10^{-11}$ for females and $p = 2 \times 10^{-11}$ for males, two-sided rank-sum comparison of sine and pulse responses).

(D) Comparison of male and female LJ responses to sine (blue) and pulse (red) stimuli. Responses to both song modes are correlated strongly for pulse ($r = 0.85$, $p = 1 \times 10^{-14}$) and moderately for sine ($r = 0.48$, $p = 0.007$) stimuli. Individual dots correspond to the average integral $\Delta F/F$ for each pulse or sine stimulus. Before averaging, the responses of each animal were normalized to compensate for inter-individual differences in calcium levels (see STAR Methods for details).

(legend continued on next page)

Hearing Pulse Song Drives Wing Extension in Males but Not in Females

Another sex-specific aspect of song responses is courtship: playback of conspecific song induces courtship-like behavior in males—this can even be directed toward other males, leading to the male chaining response, in which males chase other males while extending their wings [21, 26, 28]. In our single-fly assay, males lack a target for courtship and the song-induced arousal manifests as an increase in speed. Since FLyTRAP does not permit simultaneous recording of fly acoustic signals during playback, we quantified wing extension as a proxy for singing and examined whether song playback alone drives singing in solitary males. We found that solitary males extend their wings in response to pulse song stimuli specifically (Figures 2F and 2G; Video S2). This behavior is tuned for the IPI (similar to the locomotor response, Figure 1D)—the conspecific IPI of 36 ms drives the most wing extension, and shorter and longer IPIs evoke fewer wing extensions. By contrast, conspecific sine song (150 Hz) does not induce wing extension (Figure 2F) (see also [26, 28]). We also found that playback of pulse does not elicit wing extension in females, even though females have been shown to possess functional circuitry for singing [53, 54]—wing extension in response to pulse song is thus sex specific. These results are consistent with those for locomotor tuning: pulse song, but not sine song, generates sex-specific differences in the behavior. The identical tuning of the two behavioral responses in males (locomotion [Figure 1D] and song production [Figure 2G]) suggests that the behavioral responses are driven by a common circuit.

Drosophila Male and Female Brains Share Pulse Song Detector Neurons

Our systematic exploration of song stimulus space using the FLyTRAP assay revealed behavioral tuning for song parameters across temporal scales. We next searched for neurons with tuning across temporal scales that detect either the pulse or sine mode of courtship song. We focused on neurons expressing the Doublesex (*Dsx*) transcription factor that regulates sexual dimorphism in cell number and neuronal morphology between males and females. In the central brain there are ~70 or ~140 *Dsx*⁺ neurons per hemisphere females or males, respectively

[42, 44]. Previous studies found calcium responses to both song-like stimuli and pheromones in *Dsx*⁺ neuron projections in females [43] and tuning for the IPI in males [27]. In addition, silencing subsets of *Dsx*⁺ neurons in females affected receptivity [43]. We recorded auditory responses in *Dsx*⁺ neurons and examined tuning for song features across timescales, in both males and females, to compare with our behavioral results.

We imaged neural activity using the calcium sensor GCaMP6m [1] expressed in *Dsx*⁺ neurons. While we found no auditory response in the superior medial protocerebrum (SMP), we did find responses in the lateral junction (LJ) [55–57], a site of convergence for the majority of *Dsx*⁺ neuron projections (Figures 3A, 3B, S4B, and S4C; Video S3). Male and female *Dsx*⁺ projections in the LJ were driven strongly by pulse but not by sine stimuli (Figure 3C), confirming previous results [43]. While males produced weaker responses to auditory stimuli compared with females (Figure 3C), stimuli that evoked the strongest responses in females also evoked the strongest responses in males (Figure 3D).

The neuronal tuning curves revealed a good match between *Dsx*⁺ LJ responses and the magnitude of changes in speed across all timescales of pulse song in both sexes (Figures 3E and 3F). Results were similar whether we used the integral $\Delta F/F$ or the peak $\Delta F/F$ to quantify tuning (Figures S3F and S3G). For example, the *Dsx*⁺ LJ tuning curve for IPI is similar in females and males with the strongest responses at 36 ms, matching the behavioral tuning curves (cf. with Figures 2A, 2B, S1F, and S1G). On longer timescales, LJ tuning curves also match behavioral tuning curves for pulse train duration, with the integral calcium increasing with train duration in both sexes, similar to the behavioral response. Overall, LJ responses are tuned to multiple features found in conspecific pulse song: *Dsx*⁺ LJ responses were strongest for stimuli with a carrier frequency of 250 Hz, an IPI of 36 ms, and a pulse duration of 16 ms (Figures S3C–S3E). A mismatch in a single pulse song feature reduced calcium responses between 20% and 80% (Figure 3G). Sine stimuli have lower carrier frequencies, long durations, and no pauses (they are by definition continuous)—which explains the weak responses of *Dsx*⁺ LJ neurons to all sine stimuli (Figure 3C). Likewise, broadband noise also lacks the correct pattern of amplitude modulations and

(E) Fluorescence traces from the LJ in females (top, magenta) and males (bottom, gray) for pulse trains with three different IPIs (see legend, average over 6 individuals for each sex). In both sexes, the LJ responds most strongly to the conspecific IPI of 36 ms (Figure 1D). Responses are much weaker for shorter (16 ms) and longer (76 ms) IPIs. Calcium responses in the LJ are smaller in males than in females (cf. C). See Video S3.

(F) Tuning curves of calcium responses in the female (magenta) and the male (gray) LJ for features of pulse and sine song (cf. behavioral tuning in Figures 2A and 2B). Lines and error bars correspond to the mean \pm SEM across flies. Integral $\Delta F/F$ normalized as in (D).

(G) pC2 calcium responses to the conspecific pulse song (left), pulse song stimuli with a mismatch in a single feature (right) in males (gray) and females (magenta). A single mismatch reduces neuronal responses by at least 20% and up to 80%, indicating the high, multi-feature selectivity of pC2 in both sexes. The conspecific pulse song is shown as a reference (pulse duration 12 ms, pulse pause 24 ms, pulse carrier frequency 250 Hz, 112 pulses). Mismatch stimuli differed only in a single parameter from the reference (shortest pause: 4 ms, longest pause: 84 ms; shortest pulse: 4 ms, longest pulse: 60 ms, lowest frequency: 100 Hz, highest frequency: 800 Hz).

(H and I) Comparison of behavioral and neuronal tuning in males (H) and females (I). Behavioral and neuronal data are from flies of the same genotype (*Dsx*⁺ GCaMP). We obtained similar results when comparing the neuronal responses to behavioral data from wild-type strain NM91, Figures S3H and S3I. Each dot corresponds to the average Δ speed and the average normalized integral $\Delta F/F$ for a given pulse or sine stimulus. Lines indicate linear fits. In males (H), behavioral and neuronal responses are positively correlated for pulse (red, $r = 0.61$, $p = 1 \times 10^{-5}$) but not for sine stimuli (blue, $r = 0.17$, $p = 0.49$). In females (I), behavioral and neuronal responses are negatively correlated for pulse (red, $r = -0.53$, $p = 3 \times 10^{-4}$) but not for sine stimuli (blue, $r = 0.28$, $p = 0.25$).

All Δ speed and $\Delta F/F$ values are from *Dsx*⁺/GCaMP flies and the two measurements were made in separate individuals. (K) additionally shows behavioral data from the wild-type strain NM91. All correlation values are Spearman's rank correlation.

See also Figures S2 and S3, Video S3, and Table S1.

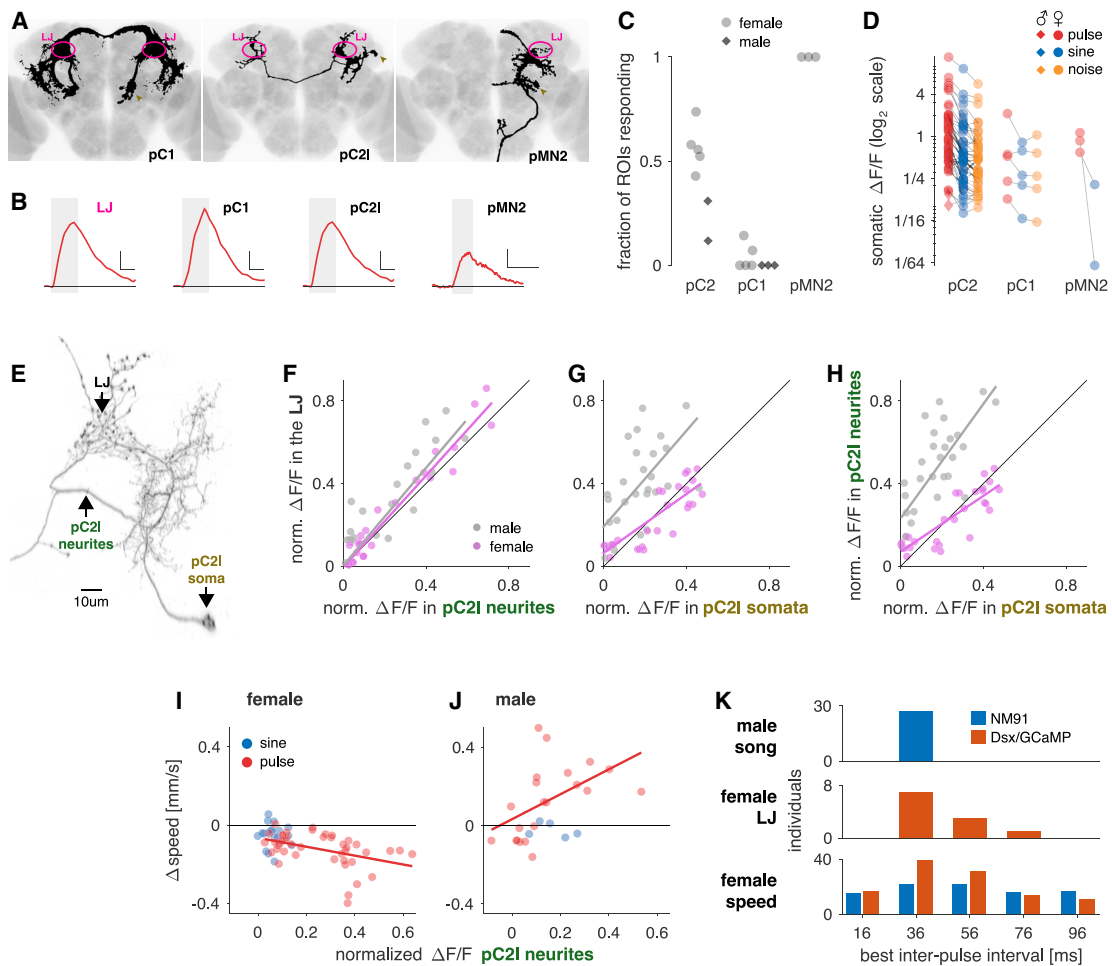


Figure 4. pC2 Neurons Are Pulse Song Detectors Common to Both Sexes

(A) Individual Dsx+ neuron types (black) with somas in the female central brain in which we detected calcium responses for pulse or sine song, registered to a common template brain (gray) (see STAR Methods for details). Of the 8 Dsx+ cell types in the central brain, pC2I, pC2m, the single female-only neuron pMN2, and a small number of pC1 neurons (and only in some individuals) respond to courtship sounds. The LJ is marked in magenta, and somata are marked with golden arrowheads.

(B) Example somatic fluorescence traces from single somata of the pC1, pC2, and pMN2 cells in response to pulse trains (IPI = 36 ms, single trial responses). Fluorescence trace from the LJ (magenta) shown for comparison. The gray box marks the duration of the sound stimulus. In each panel, horizontal and vertical scale bars correspond to 6 s and 0.25 ΔF/F, respectively. Horizontal black line marks ΔF/F = 0.

(C) Fraction of cells in Dsx+ clusters with detectable somatic calcium responses to pulse or sine song (females, light gray dots; males, dark gray squares; each dot is the fraction per fly). Complete clusters were imaged using volumetric scan for pC1, pC2, and single plane scans for pMN2. We did not distinguish between pC2I/m, since in most flies both groups are spatially intermingled at the level of cell bodies. Note that all flies included showed calcium responses to sound in the LJ, even when we did not detect responses in specific somata.

(D) Peak somatic ΔF/F for pulse (red, 36 ms IPI), sine (blue, 150 Hz), and noise (orange, 100–900 Hz). Dots correspond to the trial average for each fly. Lines connect responses recorded in the same animal. Note that responses are plotted on a log scale—the average of the ratio between sine and pulse for all cells is ~2.6. 36/38 pC2, 4/5 pC1, and 2/2 pMN2 prefer pulse over sine. See also Video S4.

(E) High-resolution confocal scan of a single pC2I neuron (obtained via a stochastic labeling technique, see STAR Methods for details). Only the side ipsilateral to the cell body is shown. The neurites in the LJ appear varicose, indicating that they contain pre-synaptic sites.

(F) Normalized integral ΔF/F values recorded simultaneously in the LJ, and the neurites that connect the LJ with the somata of pC2I (and no other Dsx+ cell type) are highly correlated in females (magenta, $r = 0.99$, $p = 1 \times 10^{-71}$, $n = 10\text{--}24$ flies/stimulus) and males (gray, $r = 0.75$, $p = 4 \times 10^{-13}$, $n = 1\text{--}6$ flies/stimulus). Each point corresponds to an individual stimulus (pulse or sine) averaged over flies. The high correlation indicates that calcium responses in the LJ reflect responses in pC2I neurons. Magenta and gray lines in (F)–(H) correspond to a least-squares fit to the individual data points.

(G) Normalized integral ΔF/F recorded first in the LJ and then in single pC2I somata in the same fly are highly correlated in both sexes (females: $r = 0.86$, $p = 8 \times 10^{-10}$, $n = 8$ flies/stimulus, males: $r = 0.73$, $p = 4 \times 10^{-6}$, $n = 1$ fly/stimulus), demonstrating that calcium responses in the LJ represent the responses of individual pC2I cells, with some variability across individual cells and animals.

(H) Normalized integral ΔF/F responses from the pC2I neurites and from single pC2I somata in different flies are highly correlated in both sexes (females: $r = 0.89$, $p = 2 \times 10^{-11}$, $n = 8$ flies/stimulus, males: $r = 0.79$, $p = 1 \times 10^{-7}$, $n = 1$ fly/stimulus). The pC2I neurites reflect the average activity of individual pC2I neurons, with some variability across individual cells and animals.

(legend continued on next page)

accordingly does not strongly drive the Dsx+ LJ neurons (see also Figure 4D). Given this tuning for the features defining conspecific pulse song, it is unlikely that the LJ would be driven by other naturally occurring stimuli: wind stimuli typically contain lower frequencies [58] and lack the periodical pattern of pulse trains required to strongly drive Dsx+ LJ neurons, and aggression song differs from courtship pulse song in carrier frequency and in IPI [59].

To more directly show that Dsx+ LJ neurons are shared pulse song detectors, we matched neuronal and behavioral responses for the same stimuli. Given the strain dependence of behavioral responses in FlyTRAP (Figure S1E), we compared behavioral and neuronal tuning within the same genotype (Dsx/GCaMP). In FlyTRAP, Dsx/GCaMP flies produced weaker behavioral responses, but nonetheless their tuning for song features was matched to that of wild-type strain NM91 (Figures S1F–S1I; Table S1). Male neural and behavioral tuning for pulse stimuli are positively correlated ($r = 0.61$, $p = 1 \times 10^{-5}$)—high Dsx+ LJ neuron activity correlates with the most acceleration (Figure 3H). Female neural and behavioral tuning for pulse stimuli are negatively correlated ($r = -0.53$, $p = 3 \times 10^{-4}$)—high Dsx+ LJ neuron activity correlates with the most slowing (Figure 3I). This suggests that these neurons control the magnitude, but not the direction, of speed changes. We observed no statistically significant correlation for sine stimuli (male: $r = 0.17$, $p = 0.49$; female: $r = 0.28$, $p = 0.25$), as Dsx+ LJ responses to sine stimuli were weak. We obtained a similar pattern of correlations when using behavioral data from the wild-type strain NM91 for comparison (Figures S3H and S3I). Notably, Dsx+ LJ activity only accounts for roughly 1/3 of the variability in behavioral responses for pulse song. This suggests that the behavior is driven and modulated by additional pathways parallel to or downstream of the Dsx+ neurons in the LJ. Nonetheless, Dsx+ neurons that innervate the LJ have tuning properties expected for pulse song detectors—they prefer pulse over sine stimuli and are similarly tuned in males and females, and their feature tuning matches the behavioral tuning for all pulse, but not sine, stimuli across timescales.

Dsx+ pC2 Neurons Are Tuned Like the LJ and to Conspecific Pulse Song

The Dsx+ neurons of the central brain form a morphologically heterogeneous population with several distinct, anatomical clusters many of which project to the LJ [27, 42, 43, 44] (Figure 3A). Previous studies that examined auditory responses in Dsx+ neurons [27, 43] did not resolve which subtype carried the response.

Using a stochastic labeling approach [60], we confirmed that five out of eight Dsx+ cell types in the female brain have projections into the LJ [44]: pC1, pC2l/m, pMN1, and pMN2, but not pC1d/m and aDN (Figures 4A, S4D, and S4E). We next imaged calcium responses to pulse and sine stimuli in the somas of all five Dsx+ cell types that innervate the LJ and found that a subset of neurons in the pC1 and pC2l/m clusters possess auditory responses, in addition to cell type pMN2 (a ventral nerve cord-projecting female-specific neuron [44] comprising only one cell body per hemisphere) (Figures 4B and 4C; Video S4). All responsive cells preferred pulse over sine or noise stimuli (Figure 4D). We did not observe auditory responses in pMN1 neurons (data not shown), although we cannot rule out that this neuron class has responses that are below the level of detection by the calcium indicator GCaMP6m.

The pC1 cluster—which was previously considered the only Dsx+ auditory neuron in the LJ [27, 43]—contained very few somas with calcium responses to sound (2–3 cells in the female brain; none in the male brain) (Figure 4C). By contrast, we found ~15 auditory neurons in the pC2 cluster in each animal (this number is likely an underestimate since somas overlap; see STAR Methods). While pC1 and pMN2 likely contribute to the LJ responses, they contain few auditory-responsive neurons and/or are present only in females. We therefore focused on pC2 as the putative pulse song detector common to both sexes.

Although there are more pC2 neurons in males versus females (~67 versus ~26, [44]) the number of auditory neurons is similar in both sexes (~15). pC2 neurons can be subdivided into a lateral and a medial type, termed pC2l and pC2m [61], and each type projects to the LJ via a distinct bundle of neurites (see Figures 3A, S4B, and S4C). Most auditory neuron somas were lateral in the pC2 cluster in both sexes (Figure S4A), and pC2l neurites produced strong auditory responses. However, we did observe auditory responses from some pC2m neurons indicating that auditory activity is not exclusive to pC2l (Figure S4A). While tuning differed slightly between individual pC2 neurons, no single cell was specialized to detect specific features of the pulse song (Figure S4F) and responses of single cells and the LJ were highly correlated in both sexes (Figures 4F–H). From this, we conclude that LJ responses reflect the tuning of pC2l neurons. Importantly, the tuning of the pC2l neurites in the LJ matches the behavioral tuning in both sexes (Figures 4I, 4J, S4G, and S4H), indicating that pC2l neurons are tuned for conspecific pulse song.

(I and J) Comparison of calcium responses in the pC2l neurites and male (I) or female (J) speed for the same stimuli. Calcium and speed data come from different flies of the same genotype (Dsx/GCaMP). Similar results were obtained when using speed data from wild-type flies (NM91) instead (Figures S4G and S4H). pC2l and behavioral responses are highly correlated for pulse with a sex-specific sign (female, I: pulse: $r = -0.49$, $p = 1 \times 10^{-3}$, sine: $r = -0.09$, $p = 0.73$; male, J: pulse: $r = 0.70$, $p = 5 \times 10^{-4}$, sine: $r = -0.20$, $p = 0.78$), just as for the LJ (cf. Figure 3I). The match between neuronal and behavioral tuning for pulse song indicates that pC2l neurons detect the pulse song. Each point corresponds to the average response to an individual pulse or sine stimulus (Δ speed: $n \sim 100$ flies per stimulus, $\Delta F/F$: $n = 10\text{--}24$ female and 1–6 male flies/stimulus).

(K) Comparison across individuals of most frequent IPIs in male song ($n = 75,528$ pulses from 27 males) and preferred IPIs in the female LJ (integral $\Delta F/F$; $n = 11$ females) and behavior (Δ speed; $n = 112$ females NM91 and 92 females Dsx/GCaMP). Song and speed are shown for NM91 (blue); LJ and speed are shown for Dsx/GCaMP (orange). While all males produce songs with IPIs around 36 ms, female neuronal and behavioral tuning for IPI is much more variable (SDs: 2.4 ms for male song, 14 ms for female $\Delta F/F$ [for integral $\Delta F/F$ (shown), 7 ms for peak $\Delta F/F$], 23 and 27 ms for the speed of NM91 and Dsx/GCaMP females, respectively). Notably, variability in female speed is larger than in the female LJ, indicating that pathways parallel to or downstream of the LJ contribute to the behavior.

All Δ speed and $\Delta F/F$ values are from flies expressing GCaMP6m under the control of Dsx-Gal4 and were measured in separate individuals. All correlation values are Spearman's rank correlation. See also Figure S4, Video S4, and Table S1.

Circuits Parallel to or Downstream of pC2I Strongly Contribute to Behavioral Variability

The match between behavioral and pC2 tuning suggests that pC2 contributes to the sex-specific responses to song. If locomotor responses were driven mainly and directly by pC2, then the variability in pC2 tuning across animals would explain most of the variability in behavioral responses across animals. On the other hand, if locomotor responses were controlled by parallel pathways or by circuits downstream of pC2, then the variability in pC2 would be much lower than the behavioral variability across animals. We compared individual variability of male song, female pC2 neural responses, and female locomotor responses (Figure 4K) and focused on IPI. We found a steady increase in variability from song to brain to behavior. Song is consistent across individuals. pC2 (LJ) responses are more variable than song but still relatively consistent across animals. By contrast, behavioral responses are highly variable—only half of the flies slow most strongly to IPIs between 36 and 76 ms. Variability at the level of locomotor responses increases for other song features, too (data not shown). Overall, this suggests that locomotor responses in FLyTRAP are strongly affected by pathways parallel to or downstream of pC2. This must be considered when interpreting experiments that test the role of pC2 in driving behavioral responses to song.

Activation and Inactivation of pC2I Neurons Affects Sex-Specific Behaviors

Given that pC2I neurons are tuned to the conspecific pulse song, we expected that their activation could also contribute to the sex-specific behaviors observed for pulse song—changes in locomotion and singing that are distinct between males and females. To test this hypothesis, we used a driver line [43, 54] that labels 11/22 female and 22/36 male pC2I neurons, in addition to 5–6 pCd neurons but no pC2m or pC1 neurons (Figure S5A). At least 5 of the pC2I cells in this driver line responded to song (Figure S5B), which corresponds to ~1/3 of the auditory pC2I neurons. We expressed CsChrimson, a red-shifted channelrhodopsin [62], in these neurons and optogenetically activated them in both males and females.

We first recorded behavior in a chamber tiled with microphones [15] to test whether pC2 activation was sufficient to induce singing (see Figures 2F and 2G). Upon red light activation, males produced pulse song, while sine song was produced transiently after stimulus offset (Figure 5A; Video S5), and the amount of pulse song produced scaled with the strength of activation (Figure 5B). The evoked pulse and sine songs were virtually indistinguishable from natural song (Figures S5C and S5D). In *Drosophila*, retinal (the channelrhodopsin cofactor) must be supplied via feeding, and red-light stimulation drove singing significantly more in males fed with retinal versus those fed regular food (Figure S5E). Activation of a control line that only labels pCd neurons [43] did not drive singing (Figure S5E), implying that song production results from the activation of the pC2 neurons in our driver. Importantly, we never observed song production upon pC2 activation in females (Figures 5D and 5E)—pC2 neurons thus drive song in a sex-specific manner. These results also establish pC2 neurons as serving a dual sensory and motor role: they respond more strongly to the

pulse song (Figures 3C and 3F) and also bias the song pathway toward producing the same song mode (Figures 5A and 5B).

We next tested whether inactivation of pC2 affected song production during courtship, by constitutively suppressing the synaptic output of pC2 (via expression of TNT [63]) in males courting wild-type virgin females (see STAR Methods). Males with a genetically silenced subset of pC2 neurons still sang wild-type-like pulse song with normal IPIs, pulse shapes, and carrier frequencies (Figures S5F and S5G)—copulation rates were also normal (Figure S5H). However, pC2I-silenced males sang about twice as much as the controls, and this effect was largely driven by the production of more sine song (Figure 5F). Given that pC2 activation yielded virtually no sine song during optogenetic stimulation (Figures 5A and 5B), this suggests that pC2 inhibits sine song production during natural courtship and generally demonstrates that song production in *Drosophila* involves a complex control scheme (see also [17, 64, 65]).

To test whether pC2 activation can produce sex-specific locomotor responses, we placed flies in the FLyTRAP assay and used red light for activation (instead of sound). Given the genotype dependence of the locomotor tuning, we expressed csChrimson in pC2 using two different genotypes. Both carried the same transgenes for expressing csChrimson in pC2 neurons, but one carried half of its chromosomes from the NM91 wild-type strain—these genotypes are called “pC2I-csChrimson” and “pC2I-csChrimson/NM91” (see STAR Methods). Both strains produced song upon optogenetic activation in males but not in females (Figures 5A–5E, S5I, and S5J). In FLyTRAP, these strains produced different but nonetheless sex-specific locomotor responses for IPI stimuli (Figure S1E), allowing us to test whether locomotor responses evoked by pC2 activation are robustly sex specific despite genotype-specific locomotor tuning. To account for innate visual responses to the light stimulus, we subtracted the responses of normally fed flies from retinal fed flies (Figures S6A and S6B).

For both strains, optogenetic activation of pC2 yielded sex-specific locomotor responses. For pC2I-csChrimson, we observed complex, multiphasic locomotor dynamics, with males tending to slow down and females tending to speed up with increasing optogenetic activation (Figures 5G and 5H). For pC2I-csChrimson/NM91, we observed simpler, bi-phasic responses—females first sped up during activation and slowed down after, while males sped up for a short period after stimulation onset only (Figure 5J). For this genotype, responses differed little across activation levels (Figure 5K). Importantly, locomotor responses were sex specific in both genotypes, which we confirmed using principal-component analysis (PCA) of the speed traces of males and females (Figures 5I and 5L). The first two principal components were sufficient to explain 80% and 99% of the variance in the speed traces, and the responses occupy non-overlapping regions in the principal component space. However, pC2 activation in neither strain reproduced the responses to pulse trains of varying IPI (for the same strain) in FlyTRAP (cf. Figure S1E). This could be because the pC2 activation levels were not matched in optogenetic experiments versus playback experiments or because song activates multiple circuits that all affect the locomotor responses. Nonetheless, the results show that pC2 is one of several elements that contribute to the locomotor tuning for song.

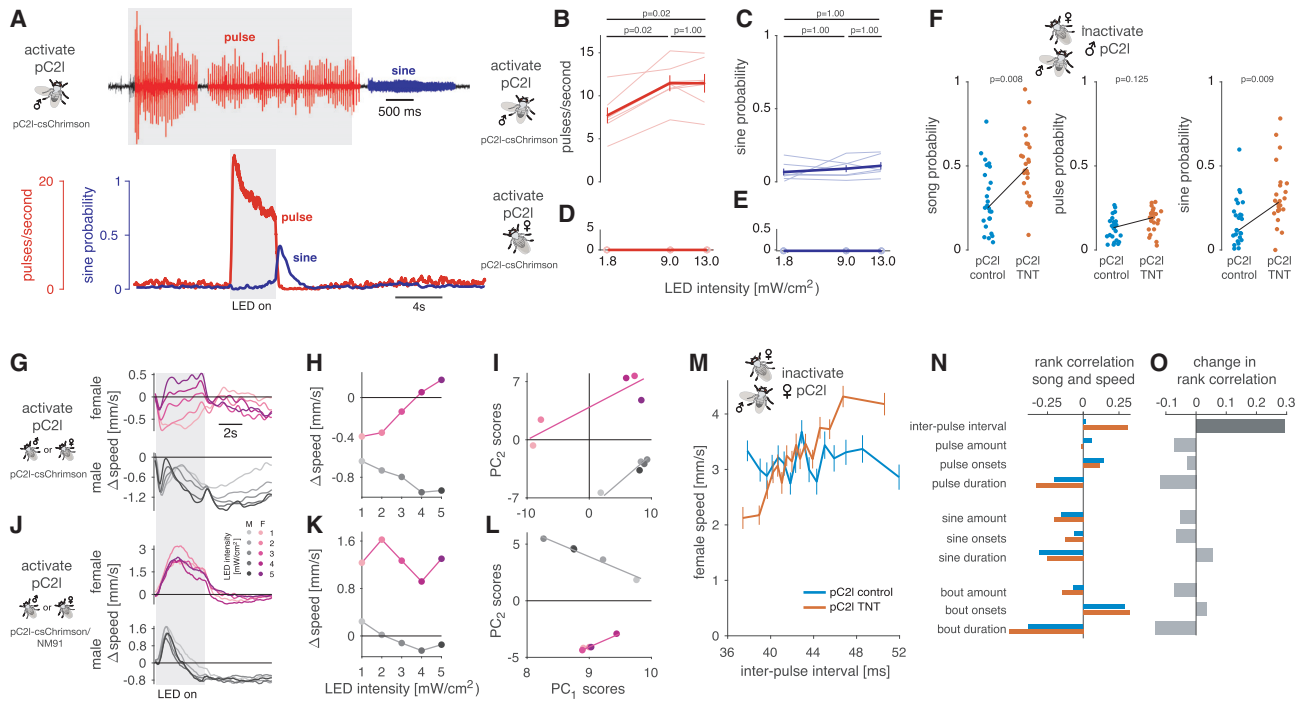


Figure 5. Testing the Necessity and Sufficiency of pC2 Neurons for Song and Locomotor Behaviors

(A) Song evoked in males by optogenetic activation (627 nm LEDs, intensity 13 mW/cm^2) of a driver line that labels pC2I and pCd neurons ($R42B01 \cap Dsx$, referred to as pC2I-csChrimson). Top trace shows a song recording marking pulse and sine song in red and blue, respectively. The gray area indicates the duration (4 s) of optogenetic activation. Pulse song is evoked during activation while sine song occurs immediately following activation. Bottom plots show pulse rate (red) and sine song probability (blue) averaged over 7 flies (18 stimulation epochs per animals). See Video S5. Activation of pC2I using a different genotype (pC2I-csChrimson/NM91) has similar effects (Figures S6A and S6B)

(B and C) Average pulse rate (B) and sine song probability (C) evoked in the 6 s following LED light onset (LED duration is 4 s). Dose-response curves for individuals are shown as thin lines; population averages ($\text{mean} \pm \text{SEM}$) are shown as thick lines with error bars. p values result from two-sided sign tests and are adjusted for multiple comparisons using Bonferroni's method. Same data as in (A) are shown.

(D and E) Same as (B) and (C) but for females ($n = 3$ flies). Activation of pC2I (and pCd) in the female does not evoke song—pC2I activation drives singing in a sex-specific manner.

(F) Song of males courting wild-type NM91 females. pC2I synaptic output in the males was inhibited using TNT via the $R42B01 \cap Dsx$ driver. Dots correspond to the amount of all song (left), pulse song (middle), and sine song (right) per fly (pC2I TNT ($n = 24$)—orange, pC2I control ($n = 25$)—blue). Black lines connect the means of the two genotypes. p values show the outcome of a two-sided rank-sum test. Inhibiting pC2I output leads to more overall singing and sine song, but not to more pulse song, indicating that pC2I biases singing toward pulse song during courtship. Other song features are not affected (see Figures S5F and S5G).

(G and H) Optogenetic activation of $R42B01 \cap Dsx$ using csChrimson (pC2I-csChrimson) evokes locomotor responses with sex-specific dynamics. Changes in speed (G) and tuning curves (H) were corrected for intrinsic light responses by subtracting the responses of control flies with the same genotype that were not fed retinal (see Figure S6A). Females (top, magenta) slow for weak and speed for strong activation with multi-phasic dynamics. Males decrease their speed and responses outlast the optogenetic stimulus (bottom, gray). See Figure S6A for n flies. The gray area indicates the duration of LED stimulation (4 s).

(I) Principal-component analysis (PCA) of male and female locomotor speed traces (12 s following stimulus LED or sound onset, traces taken from G). Shown are first and second principal-component (PC) scores of females (magenta) and males (gray) for sound (squares) and optogenetic stimulation (circles). Lines correspond to linear fits for each sex. Female and male responses to different LED occupy different areas in PC space, indicating that the locomotor dynamics are sex specific.

(J and K) Same as (G) and (H) but with a different genotype (pC2I-csChrimson/NM91—see STAR Methods for details). Females (top, magenta) speed throughout the stimulation (J) and for all LED intensities (K). Males (bottom, gray) first speed and then slow for all LED intensities. The evoked locomotor dynamics differ between genotypes (I) but are always sex specific.

(L) Same as (I) but with the pC2I-csChrimson/NM91 phenotype. Again, male and female locomotor responses are different, since they occupy different regions in PC space (compare [I]).

(M) Locomotor tuning for inter-pulse interval during natural courtship obtained from single females that were courted by a wild-type NM91 male. pC2I synaptic output in the females was inhibited with TNT using the $R42B01 Dsx$ driver. Lines and error bars correspond to the mean \pm SEM speed over 48 females per genotype tested (pC2I TNT—orange, pC2I control—blue, see methods for details on how the tuning curves were computed). pC2I control females (blue) do not change their speed with IPI within the range commonly produced by males ($r = 0.02$, $p = 0.59$, compare Figure 1D). pC2I TNT females (orange) accelerate for longer IPIs ($r = 0.31$, $p = 3 \times 10^{-30}$).

(N) Rank correlation between female speed and different song features during natural courtship (pC2I control—blue, pC2I TNT—orange).

(O) Difference between the rank correlations for control (blue) and pC2I TNT (orange) flies in (N). pC2I inactivation specifically changes the correlation between female speed and IPI (dark gray, $p = 6 \times 10^{-8}$). All other changes in correlation are much smaller and not significant ($p > 0.18$). p values were obtained by fitting an ANCOVA model (see methods for details) and were corrected for multiple comparisons using the Bonferroni method. All correlation values are Spearman's rank correlation. See also Figure S5 and Video S5.

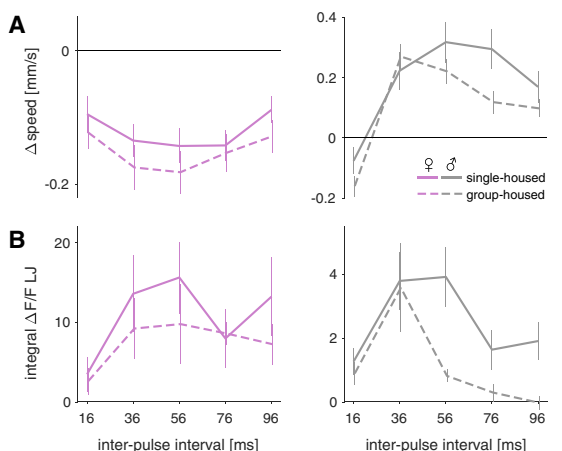


Figure 5. Behavioral and pC2 Responses Are Modulated by Social Experience
(A) Changes in speed for pulse trains measured using FLyTRAP with different IPIs in single-housed (solid line) or group-housed (dashed lines) female (left, magenta) and male flies (right, gray). Plots show mean \pm SEM across 92/116 group-housed and 137/71 single-housed female/male flies. Female IPI tuning is not strongly affected by housing conditions. By contrast, males change their speed more selectively when group housed.
(B) Calcium responses from the LJ for pulse trains with different IPIs in single-housed (solid line) or group-housed (dashed lines) female (left, magenta) and male flies (right, gray). Plots show mean \pm SEM across 5–6 female or male flies in each condition. In females, group housing only weakly suppresses LJ responses for some IPIs. By contrast, male LJ responses are selectively suppressed for long IPIs, which sharpens the IPI tuning.
(C) Ratio of calcium responses to 36 and 56 ms IPIs in single-housed or group-housed female (left, magenta) and male flies (right, gray). Individual dots correspond to individual flies; the solid lines connect the population average ratios.
 p values were obtained from a two-sided Wilcoxon rank-sum test. All Δ speed and $\Delta F/F$ values are from flies expressing GCaMP6m under the control of Dsx-Gal4, and the two measurements were made in separate flies. See also Figure S6.

Finally, we used the pC2I-TNT driver to constitutively suppress the synaptic output of pC2 in females and paired them with wild-type virgin males (see STAR Methods). We quantified female song responses as the correlation between different song features and female speed [15, 19] (Figures 5M–5O). Because male song is structured via sensory feedback cues from the female [15], silencing pC2 neurons in females could affect the content of male song—however, the statistics of male song were unchanged by the female manipulation (Figures S6C and S6D). pC2 inactivation specifically affected the correlation between female speed and the pulse song IPI, which changed from ~ 0 to $+0.3$ (Figures 5M–5O). While control—and wild-type [19]—females do not change their speed relative to the range of natural IPIs produced by conspecific males (Figure 1), females with pC2 neurons silenced accelerate more with increasing IPI. pC2 neurons are therefore required for the normal response to pulse song. The remaining responses to pulse could be caused by pC2 neurons not silenced by our genetic driver or by other neurons tuned for longer IPIs [27]. While female locomotor responses to courtship song were affected by pC2 inactivation, copulation rates were not significantly reduced (Figure S6E), consistent with previous studies [43]. In conjunction with the match between behavioral tuning and pC2 tuning (Figures 3H and 3I), these results add to the evidence that pC2 neurons detect pulse song and play a critical role at the sensorimotor interface—they relay information about pulse song to sex-specific downstream circuits that control either singing or locomotion, and thereby contribute to acoustic communication behaviors.

Auditory Responses of pC2 Are Modulated by Social Experience

Social experience is also known to affect courtship behavior in *Drosophila* [21, 66, 67]. In particular, a recent study has shown that group housing sharpens the IPI selectivity of the female mating decision and of the male chaining response, and that this effect is mediated by the exposure to song from other flies in the group [29]. However, we do not yet know which elements in

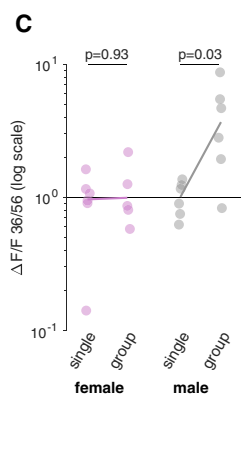


Figure 6. Behavioral and pC2 Responses Are Similarly Modulated by Social Experience

(A) Changes in speed for pulse trains measured using FLyTRAP with different IPIs in single-housed (solid line) or group-housed (dashed lines) female (left, magenta) and male flies (right, gray). Plots show mean \pm SEM across 92/116 group-housed and 137/71 single-housed female/male flies. Female IPI tuning is not strongly affected by housing conditions. By contrast, males change their speed more selectively when group housed.
(B) Calcium responses from the LJ for pulse trains with different IPIs in single-housed (solid line) or group-housed (dashed lines) female (left, magenta) and male flies (right, gray). Plots show mean \pm SEM across 5–6 female or male flies in each condition. In females, group housing only weakly suppresses LJ responses for some IPIs. By contrast, male LJ responses are selectively suppressed for long IPIs, which sharpens the IPI tuning.

the pathway from song to behavior are affected by social experience. Given that pC2 contributes to behavioral responses to song, we asked whether its activity is modulated by housing conditions. The behavioral results presented so far were obtained from group-housed flies so we also ran single-housed males or females to confirm that locomotor responses in FLyTRAP are modulated by social experience. We found that single-housed males responded with little selectivity to pulse trains with different IPIs (Figure 6A). This is consistent with the previous study [29], since group-housed males are exposed to the song of other males during rearing. That we can reproduce these results in a single-fly assay shows that acoustic cues are sufficient to express the effect—previous experiments had used multi-fly assays, leaving open the possibility of other cues being required. By contrast, females do not sing to other females, and, accordingly, their locomotor responses are unaffected by the housing condition. Consistent with the behavior, calcium responses in pC2 (measured via the LJ) (Figures 4F–4H) do not change strongly with housing conditions in females but become more selective for IPI in group-housed males (Figures 6B and 6C). Notably, responses to sine song and to pulse trains with different durations are not affected by housing conditions (Figures S6F and S6G). This suggests that pC2 could mediate the effect of social experience on the behavioral responses to song.

DISCUSSION

Using a quantitative behavioral assay, we characterized locomotor responses in both males and females to the features of the *Drosophila melanogaster* courtship song. Males and females showed similar tuning for pulse song, but nonetheless produced distinct responses (males accelerate while females decelerate; males sing while females do not) (Figures 1 and 2). For both males and females and across multiple timescales, tuning was matched to the distribution of each parameter in the male's pulse song. We then identified Dsx+ pC2 neurons in the brain that respond strongly to all features of pulse song, and whose tuning

is matched to behavioral tuning (Figures 3 and 4). The activation of pC2 neurons elicited sex-specific behavioral responses to pulse song (Figure 5), and social experience sharpened both behavioral selectivity and pC2 tuning (Figure 6). We thus conclude that Dsx+ pC2 neurons connect song detection with the execution of sex-specific behaviors.

Matches between Behavioral Tuning and Conspecific Song

In FLyTRAP, locomotor tuning in NM91 and Dsx/GCaMP females overlaps with the conspecific song—these females slow to conspecific song (Figures 2A, S1F, and S1H) and do not change their speed or may even accelerate for deviant pulse parameters (Figures S2A and S2E). However, the tuning for any single song feature is not sufficiently narrow to serve as an effective filter for conspecific song. For instance, NM91 and Dsx/GCaMP females also slow for IPIs produced by a sibling species *D. simulans* (50–65 ms) [45]. However, *D. simulans* pulses would be rejected based on a mismatch in other song features—*D. simulans* pulses are too short and of too high frequency to be accepted by females [17, 68]. Combinatorial selectivity for multiple song features may thus enable species discrimination with broad single-feature tuning [34]. Males and females are exposed to additional cues during courtship that may further sharpen behavioral tuning. For instance, chemical cues prevent males from courting heterospecific females [69] and likely also contribute to female rejection [5, 47]—it will be interesting to explore how non-auditory cues [70, 71] modulate locomotor responses to song and whether multi-modal integration occurs in pC2 neurons or elsewhere. The absence of non-acoustic cues may explain the diversity of locomotor responses across strains in the FLyTRAP assay (Figure S1E).

In contrast to pulse song responses, the locomotor and singing responses for sine song in FLyTRAP were less sex specific (Figure 2E), and the behavioral tuning did not match well the conspecific song—very low frequencies never produced by males slowed NM91 females the most (Figure 2A). This implies divergent roles for the two song modes and is consistent with previous studies [26, 51]—for instance, sine song does not induce male-male courtship [28]. It has been suggested that pulse song may modulate sine song responses [51], but we did not detect strong serial interactions between the two song modes (Figure S2G). Alternatively, responses to sine song may depend more strongly on the presence of male chemical cues [4, 5] that are absent in the FLyTRAP assay. This is consistent with sine song being produced when the male is near the female [15]—that is, when these chemical cues are particularly strong.

Pathways for Detecting Sine and Pulse

Our behavioral and neuronal results suggest that pulse and sine song are processed in parallel pathways (Figures 2E, 3C, and 3F–3I), but it is unclear as of yet how and where sounds are split into different streams. Sine and pulse can be separated based on spectral and temporal properties. In fact, the frequency tuning in auditory receptor neurons (JON) and first-order auditory brain neurons (AMMC) may already be sufficient to separate the lower-frequency sine (150 Hz) from the higher-frequency pulse (>220 Hz) [72–76]. The temporal pattern could further discriminate pulse from sine by either suppressing responses to the

sustained sine via adaptation or by tuning temporal integration such that the brief pulse stimuli fail to drive neuronal spiking. Recently, a comprehensive mapping of auditory activity throughout the *Drosophila* brain revealed diverse responses to sine and pulse stimuli in many brain regions not previously known to be part of the auditory pathway [77]. Future work will need to determine how such diverse and widespread responses are combined to generate the kind of feature selectivity present in pC2 neurons.

Our data indicate that pC2 neurons are not the only neurons used to detect pulse song, since the variability of pC2 neurons across stimuli and individuals does not account for the full behavioral variability (Figures 3H, 3I, and 4I–4K). Interestingly, previous studies have implied pC1 as a pulse song detector [27, 43]. Like pC2, pC1 exists in males and females [2], and activation drives several courtship-related behaviors in males—including singing, male-male courtship, and aggression [27, 64, 78–80]—and also in females [29, 43, 54]. All previous studies have relied on imaging activity in the LJ to show that pC1 preferentially responds to pulse song [27, 43]. However, we show here that calcium responses of Dsx+ neurons in the LJ reflect the auditory activity of multiple Dsx+ cell types—and we detected auditory responses in the somas of pC2, pC1 (only in females), and pMN2 (a female-only neuron) (Figure 4). Because the number of auditory neurons within the pC2 cluster is much larger than for pC1 or pMN2 (Figure 4C), and because tuning in pC2 somas matches the tuning in the LJ (Figures 4E–4H), we conclude that the LJ activity largely reflects pC2 responses. Nonetheless, we have not exhaustively assessed the match between the neuronal responses of female pC1 and pMN2 neurons and behavior. Those neurons may also be critical for the female's response to pulse song, including behaviors not investigated here (such as oviposition [44]).

Inputs and Outputs of pC2 Neurons

pC2 neurons bind different properties of the pulse song to selectively signal the presence of conspecific pulse song (Figures 3 and S3C–S3E). How this selectivity arises is as of yet unclear since systematic studies of tuning for multiple pulse song features in the early auditory pathway are missing. However, existing evidence suggests that pC2 may acquire its tuning in a serial manner—via a cumulative sharpening of tuning for song features at successive stages of auditory processing [25, 27, 43, 72, 74, 75, 81], via resonant conductances [76], adaptation [82], or through the interplay of excitation and inhibition [81]. This serial sharpening is similar to how selectivity for pulse song arises in crickets, in which a delay-line and coincidence detector mechanism produces broad selectivity for pulse duration and pulse pause, which is subsequently sharpened in a downstream neuron [83]. More direct readouts of the membrane voltage of auditory neurons in the fly brain are required to determine the biophysical mechanisms that generate song selectivity in pC2.

Similarly, the circuits downstream of pC2 neurons that control the diverse and sex-specific behaviors reported here remain to be identified. Our assessment of inter-individual variability in IPI preference revealed that most of the behavioral variability does not arise at the level of pC2 neurons (Figure 4K). This suggests that variability in parallel or in downstream pathways

strongly contributes to the locomotor tuning—pC2 activity is only one of multiple determinants of the behavior. pC2 neurons may connect directly with descending interneurons (DNs) [84, 85] that control motor behaviors. For example, pC2 activation in males drives pulse song production, followed by sine song production at stimulus offset (Figure 5A). This behavior resembles that caused by pIP10 activation [17]—pIP10 is a male-only descending neuron [64], but we don't yet know whether it directly connects with pC2 neurons. Notably, song also promotes copulation in females, but we did not detect a significant effect of pC2 inactivation on copulation rates (Figure S6E). This suggests that parallel pathways integrate song on different timescales to control the mating and locomotor responses to song [19, 86], respectively.

Modularity Facilitates Plasticity of Behavioral Responses to Song

Our behavioral data suggest that some aspects of the sex specificity of behavior arises after feature tuning. The pC2 neurons are selective for pulse song in both sexes (Figures 3 and 4) and drive locomotor responses with sex-specific dynamics or singing in males (Figure 5). This is reminiscent of how sex-specific behaviors are driven to the male pheromone cVA in flies: shared detector neurons—olfactory receptor neurons and projection neurons in the antennal lobe—detect cVA in both sexes, and this information is then routed to sex-specific higher-order neurons in the lateral horn, which are thought to drive the different behaviors [6–8]. This modular architecture with detectors of social signals being flexibly routed to different behavioral outputs is beneficial if these routes are plastic. For instance, here we show that social experience can shape male responses to song (similar to [29]), along with tuning at the level of the neurons that detect the song (Figure 6). During mating, males transfer a sex peptide to females [87] that alters female behavioral responses to song from slowing to acceleration [15]—these effects may arise at the level of the motor circuits downstream of pC2, shifting pulse song responses in females to resemble those of males. Modularity also facilitates behavioral plasticity on evolutionary timescales since only one element—the feature detector—needs to change for behavioral tuning in both sexes to adapt to new songs that evolve during speciation [88, 89]. The identification of pC2 neurons as pulse song detectors will therefore benefit future studies of the evolution of song recognition.

pC2 Neurons Have a Dual Sensory and Motor Role

Unlike regular higher-order sensory neurons, which detect a sensory cue to produce different behaviors, pC2 neurons detect the cue whose production they drive (Figures 3F, 3G, and 5A–5C). Such a dual sensory and motor role may guide social interactions and communication via imitation. In *Drosophila melanogaster*, hearing the song of other males induces a male to court and sing to other females and even males [26, 28]. This behavior may have originated because the song of another male indicates the presence of a female nearby.

Neurons with a dual sensory and motor roles are well-known from vertebrates [90–92]. For instance, “mirror” neurons are active during the production as well as the observation of a behavior and are thought to be crucial for imitation learning and communication between conspecifics [93]. Neurons with a

sensorimotor correspondence in the brain of song birds are active during singing and hearing song, and these neurons are hypothesized to play a role in song learning [91]. Importantly, pC2 differs crucially from these instances in that it directly drives the production of the acoustic signal it detects (Figures 5A–5C). Because we recorded pC2 activity in passively listening males, we do not yet know whether pC2 is activated by sound in an actively singing male. If so, hearing its own song could induce self-stimulation and form a positive feedback loop to maintain courtship behavior by mediating persistent behavioral state changes [94]. Alternatively, auditory inputs could be suppressed during singing via a corollary discharge [95, 96], which would allow pC2 to maintain sensitivity to the song of other males to coordinate inter-male competition during singing. Additional studies of pC2 activity in behaving animals are required to fully understand how these pulse song detector neurons integrate into the acoustic communication behavior.

In summary, we show how the circuits that recognize song to drive diverse and sex-specific behavioral responses are organized in *Drosophila*: common detector neurons—pC2—recognize pulse song in both males and females, and this identically processed information is then routed to drive multiple sex-specific behaviors. Similar principles may underlie the production of sex-specific behavioral responses to communication signals in other insects, song birds, or mammals.

STAR★METHODS

Detailed methods are provided in the online version of this paper and include the following:

- KEY RESOURCES TABLE
- LEAD CONTACT AND MATERIALS AVAILABILITY
- EXPERIMENTAL MODEL AND SUBJECT DETAILS
- METHOD DETAILS
 - FLyTRAP
 - Playback experiments
 - Stimulus design
 - Analysis of FLyTRAP data
 - Manual scoring of wing extension in FLyTRAP
 - Joint tuning for pulse duration and pause
 - Measurement of song features from song
 - PCA of speed traces
 - Optogenetic experiments
 - pC2 inactivation during courtship
 - Calcium imaging
 - Light microscopy
- QUANTIFICATION AND STATISTICAL ANALYSIS
- DATA AND CODE AVAILABILITY

SUPPLEMENTAL INFORMATION

Supplemental Information can be found online at <https://doi.org/10.1016/j.cub.2019.08.008>.

ACKNOWLEDGMENTS

We thank Isabel D'Allesandro for help with playback behavioral experiments; Alex Hammons and Nofar Ozeri-Engelhard for help with dissections for immunostaining; Diego Pacheco for help with aligning the volumetric GCaMP scans;

Robert Court and Doug Armstrong (<http://www.virtualflybrain.org>) for help with brain registration; David Stern, Ben Arthur, and Barry Dickson for discussions during the development of the FLYTRAP assay; Kai Feng and Barry Dickson for sharing the design of their playback assay chamber; Bruce Baker, Stephen Goodwin, Gerry Rubin, and Peter Andolfatto for gifts of flies; and Kristin Scott, Asif Ghazanfar, Tim Buschman, and members of the Murthy lab for feedback on the manuscript. J.C. was supported by a postdoctoral fellowship through the Princeton Sloan-Swartz Center and an Emmy Noether grant from the Deutsche Forschungsgemeinschaft (CL 596-1/1). M.M. was supported by an NIH New Innovator award (DP2), NIH NINDS BRAIN Initiative R01 NS104899, and an HHMI Faculty Scholar award.

AUTHOR CONTRIBUTIONS

D.D., J.C., and M.M. designed the study. S.Y.T. designed and built the two-photon microscope used for calcium imaging experiments. D.D., J.C., and G.G. collected data. D.D. and J.C. analyzed data and generated figures. D.D., J.C., and M.M. wrote the manuscript.

DECLARATION OF INTERESTS

The authors declare no competing interests.

Received: March 15, 2019

Revised: July 10, 2019

Accepted: August 2, 2019

Published: September 26, 2019

REFERENCES

- Yang, C.F., and Shah, N.M. (2014). Representing Sex in the Brain, One Module at a Time. *Neuron* 82, 261–278.
- Dulac, C., and Wagner, S. (2006). Genetic Analysis of Brain Circuits Underlying Pheromone Signaling. *Annu. Rev. Genet.* 40, 449–467.
- Wang, L., and Anderson, D.J. (2010). Identification of an aggression-promoting pheromone and its receptor neurons in *Drosophila*. *Nature* 463, 227–231.
- Kurtovic, A., Widmer, A., and Dickson, B.J. (2007). A single class of olfactory neurons mediates behavioural responses to a *Drosophila* sex pheromone. *Nature* 446, 542–546.
- Billeter, J.-C., Atallah, J., Krupp, J.J., Millar, J.G., and Levine, J.D. (2009). Specialized cells tag sexual and species identity in *Drosophila melanogaster*. *Nature* 461, 987–991.
- Datta, S.R., Vasconcelos, M.L., Ruta, V., Luo, S., Wong, A., Demir, E., Flores, J., Balonze, K., Dickson, B.J., and Axel, R. (2008). The *Drosophila* pheromone cVA activates a sexually dimorphic neural circuit. *Nature* 452, 473–477.
- Ruta, V., Datta, S.R., Vasconcelos, M.L., Freeland, J., Looger, L.L., and Axel, R. (2010). A dimorphic pheromone circuit in *Drosophila* from sensory input to descending output. *Nature* 468, 686–690.
- Kohl, J., Ostrovsky, A.D., Frechter, S., and Jefferis, G.S.X.E. (2013). A bidirectional circuit switch reroutes pheromone signals in male and female brains. *Cell* 155, 1610–1623.
- Haga, S., Hattori, T., Sato, T., Sato, K., Matsuda, S., Kobayakawa, R., Sakano, H., Yoshihara, Y., Kikusui, T., and Touhara, K. (2010). The male mouse pheromone ESP1 enhances female sexual receptive behaviour through a specific vomeronasal receptor. *Nature* 466, 118–122.
- Ishii, K.K., Osakada, T., Mori, H., Miyasaka, N., Yoshihara, Y., Miyamichi, K., and Touhara, K. (2017). A Labeled-Line Neural Circuit for Pheromone-Mediated Sexual Behaviors in Mice. *Neuron* 95, 123–137.e8.
- DiCarlo, J.J., Zoccolan, D., and Rust, N.C. (2012). How does the brain solve visual object recognition? *Neuron* 73, 415–434.
- Tsao, D.Y., and Livingstone, M.S. (2008). Mechanisms of face perception. *Annu. Rev. Neurosci.* 31, 411–437.
- Gentner, T.Q. (2008). Temporal scales of auditory objects underlying birdsong vocal recognition. *J. Acoust. Soc. Am.* 124, 1350–1359.
- Bennet-Clark, H.C., and Ewing, A.W. (1967). Stimuli provided by Courtship of Male *Drosophila melanogaster*. *Nature* 215, 669–671.
- Coen, P., Clemens, J., Weinstein, A.J., Pacheco, D.A., Deng, Y., and Murthy, M. (2014). Dynamic sensory cues shape song structure in *Drosophila*. *Nature* 507, 233–237.
- Coen, P., Xie, M., Clemens, J., and Murthy, M. (2016). Sensorimotor Transformations Underlying Variability in Song Intensity during *Drosophila* Courtship. *Neuron* 89, 629–644.
- Clemens, J., Coen, P., Roemschied, F.A., Pereira, T.D., Mazumder, D., Aldarondo, D.E., Pacheco, D.A., and Murthy, M. (2018). Discovery of a new song mode in *Drosophila* reveals hidden structure in the sensory and neural drivers of behavior. *Curr. Biol.* 28, 2400–2412.e6.
- Bussell, J.J., Yapici, N., Zhang, S.X., Dickson, B.J., and Vosshall, L.B. (2014). Abdominal-B neurons control *Drosophila* virgin female receptivity. *Curr. Biol.* 24, 1584–1595.
- Clemens, J., Girardin, C.C., Coen, P., Guan, X.-J., Dickson, B.J., and Murthy, M. (2015). Connecting Neural Codes with Behavior in the Auditory System of *Drosophila*. *Neuron* 87, 1332–1343.
- Aranha, M.M., Herrmann, D., Cachitas, H., Neto-Silva, R.M., Dias, S., and Vasconcelos, M.L. (2017). Apterous Brain Neurons Control Receptivity to Male Courtship in *Drosophila Melanogaster* Females. *Sci. Rep.* 7, 46242.
- Schilcher Von, F. (1976). The role of auditory stimuli in the courtship of *Drosophila melanogaster*. *Anim. Behav.* 24, 18–26.
- Cook, R.M. (1973). Courtship processing in *Drosophila melanogaster*. II. An adaptation to selection for receptivity to wingless males. *Anim. Behav.* 21, 349–358.
- Tompkins, L., Gross, A.C., Hall, J.C., Gailey, D.A., and Siegel, R.W. (1982). The role of female movement in the sexual behavior of *Drosophila melanogaster*. *Behav. Genet.* 12, 295–307.
- Crossley, S.A., Bennet-Clark, H.C., and Evert, H.T. (1995). Courtship song components affect male and female *Drosophila* differently. *Anim. Behav.* 50, 827–839.
- Vaughan, A.G., Zhou, C., Manoli, D.S., and Baker, B.S. (2014). Neural pathways for the detection and discrimination of conspecific song in *D. melanogaster*. *Curr. Biol.* 24, 1039–1049.
- Eberl, D.F., Duyk, G.M., and Perrimon, N. (1997). A genetic screen for mutations that disrupt an auditory response in *Drosophila melanogaster*. *Proc. Natl. Acad. Sci. USA* 94, 14837–14842.
- Zhou, C., Franconville, R., Vaughan, A.G., Robinett, C.C., Jayaraman, V., and Baker, B.S. (2015). Central neural circuitry mediating courtship song perception in male *Drosophila*. *eLife* 4, 11.
- Yoon, J., Matsuo, E., Yamada, D., Mizuno, H., Morimoto, T., Miyakawa, H., Kinoshita, S., Ishimoto, H., and Kamikouchi, A. (2013). Selectivity and plasticity in a sound-evoked male-male interaction in *Drosophila*. *PLoS ONE* 8, e74289.
- Li, X., Ishimoto, H., and Kamikouchi, A. (2018). Auditory experience controls the maturation of song discrimination and sexual response in *Drosophila*. *eLife* 7, e34348.
- Arthur, B.J., Sunayama-Morita, T., Coen, P., Murthy, M., and Stern, D.L. (2013). Multi-channel acoustic recording and automated analysis of *Drosophila* courtship songs. *BMC Biol.* 11, 11.
- Gentner, T.Q., and Margoliash, D. (2003). Neuronal populations and single cells representing learned auditory objects. *Nature* 424, 669–674.
- Griffiths, T.D., and Warren, J.D. (2004). What is an auditory object? *Nat. Rev. Neurosci.* 5, 887–892.
- Bizley, J.K., and Cohen, Y.E. (2013). The what, where and how of auditory-object perception. *Nat. Rev. Neurosci.* 14, 693–707.
- Amézquita, A., Flechas, S.V., Lima, A.P., Gasser, H., and Hödl, W. (2011). Acoustic interference and recognition space within a complex assemblage of dendrobatid frogs. *Proc. Natl. Acad. Sci. USA* 108, 17058–17063.

35. Ryan, M.J., Phelps, S.M., and Rand, A.S. (2001). How evolutionary history shapes recognition mechanisms. *Trends Cogn. Sci.* 5, 143–148.
36. Blankers, T., Hennig, R.M., and Gray, D.A. (2015). Conservation of multivariate female preference functions and preference mechanisms in three species of trilling field crickets. *J. Evol. Biol.* 28, 630–641.
37. Ryan, M.J., and Cummings, M.E. (2013). Perceptual Biases and Mate Choice. *Annu. Rev. Ecol. Evol. Syst.* 44, 437–459.
38. Rosenthal, G.G., and Ryan, M.J. (2011). Conflicting preferences within females: sexual selection versus species recognition. *Biol. Lett.* 7, 525–527.
39. Hennig, R.M., Blankers, T., and Gray, D.A. (2016). Divergence in male cricket song and female preference functions in three allopatric sister species. *J. Comp. Physiol. A Neuroethol. Sens. Neural Behav. Physiol.* 202, 347–360.
40. Helversen von D (1997). Recognition of sex in the acoustic communication of the grasshopper *Chorthippus biguttulus* (Orthoptera, Acrididae). *J. Comp. Physiol.* 180, 373–386.
41. Clemens, J., and Hennig, R.M. (2013). Computational principles underlying the recognition of acoustic signals in insects. *J. Comput. Neurosci.* 35, 75–85.
42. Rideout, E.J., Dornan, A.J., Neville, M.C., Eadie, S., and Goodwin, S.F. (2010). Control of sexual differentiation and behavior by the doublesex gene in *Drosophila melanogaster*. *Nat. Neurosci.* 13, 458–466.
43. Zhou, C., Pan, Y., Robinett, C.C., Meissner, G.W., and Baker, B.S. (2014). Central brain neurons expressing doublesex regulate female receptivity in *Drosophila*. *Neuron* 83, 149–163.
44. Kimura, K., Sato, C., Koganezawa, M., and Yamamoto, D. (2015). *Drosophila* ovipositor extension in mating behavior and egg deposition involves distinct sets of brain interneurons. *PLoS ONE* 10, e0126445.
45. Bennet-Clark, H.C., and Ewing, A.W. (1969). Pulse interval as a critical parameter in the courtship song of *Drosophila melanogaster*. *Anim. Behav.* 17, 755–759.
46. Lehnert, B.P., Baker, A.E., Gaudry, Q., Chiang, A.-S., and Wilson, R.I. (2013). Distinct roles of TRP channels in auditory transduction and amplification in *Drosophila*. *Neuron* 77, 115–128.
47. Rybak, F., Sureau, G., and Aubin, T. (2002). Functional coupling of acoustic and chemical signals in the courtship behaviour of the male *Drosophila melanogaster*. *Proc. Biol. Sci.* 269, 695–701.
48. Tinbergen, N. (1989). *The Study of Instinct* (Oxford University Press).
49. Hennig, R.M., Heller, K.-G., and Clemens, J. (2014). Time and timing in the acoustic recognition system of crickets. *Front. Physiol.* 5, 286.
50. Ronacher, B., Hennig, R.M., and Clemens, J. (2015). Computational principles underlying recognition of acoustic signals in grasshoppers and crickets. *J. Comp. Physiol. A Neuroethol. Sens. Neural Behav. Physiol.* 201, 61–71.
51. Schilcher, F.V. (1976). The function of pulse song and sine song in the courtship of *Drosophila melanogaster*. *Anim. Behav.* 24, 622–625.
52. Talyn, B.C., and Dowse, H.B. (2004). The role of courtship song in sexual selection and species recognition by female *Drosophila melanogaster*. *Anim. Behav.* 68, 1165–1180.
53. Clyne, J.D., and Miesenböck, G. (2008). Sex-specific control and tuning of the pattern generator for courtship song in *Drosophila*. *Cell* 133, 354–363.
54. Rezával, C., Pattnaik, S., Pavlou, H.J., Nojima, T., Brüggemeier, B., D'Souza, L.A.D., Dweck, H.K.M., and Goodwin, S.F. (2016). Activation of Latent Courtship Circuitry in the Brain of *Drosophila* Females Induces Male-like Behaviors. *Curr. Biol.* 26, 2508–2515.
55. Ito, K., Shinomiya, K., Ito, M., Armstrong, J.D., Boyan, G., Hartenstein, V., Harzsch, S., Heisenberg, M., Homberg, U., Jenett, A., et al.; Insect Brain Name Working Group (2014). A systematic nomenclature for the insect brain. *Neuron* 81, 755–765.
56. Cachero, S., Ostrovsky, A.D., Yu, J.Y., Dickson, B.J., and Jefferis, G.S.X.E. (2010). Sexual dimorphism in the fly brain. *Curr. Biol.* 20, 1589–1601.
57. Yu, J.Y., Kanai, M.I., Demir, E., Jefferis, G.S.X.E., and Dickson, B.J. (2010). Cellular organization of the neural circuit that drives *Drosophila* courtship behavior. *Curr. Biol.* 20, 1602–1614.
58. Nagel, K.I., and Wilson, R.I. (2011). Biophysical mechanisms underlying olfactory receptor neuron dynamics. *Nat. Neurosci.* 14, 208–216.
59. Versteven, M., Vanden Broeck, L., Geurten, B., Zwarts, L., Decraecker, L., Beelen, M., Göpfert, M.C., Heinrich, R., and Callaerts, P. (2017). Hearing regulates *Drosophila* aggression. *Proc. Natl. Acad. Sci. USA* 114, 1958–1963.
60. Nern, A., Pfeiffer, B.D., and Rubin, G.M. (2015). Optimized tools for multi-color stochastic labeling reveal diverse stereotyped cell arrangements in the fly visual system. *Proc. Natl. Acad. Sci. USA* 112, E2967–E2976.
61. Robinett, C.C., Vaughan, A.G., Knapp, J.M., and Baker, B.S. (2010). Sex and the single cell. II. There is a time and place for sex. *PLoS Biol.* 8, e1000365.
62. Klapoetke, N.C., Murata, Y., Kim, S.S., Pulver, S.R., Birdsey-Benson, A., Cho, Y.K., Morimoto, T.K., Chuong, A.S., Carpenter, E.J., Tian, Z., et al. (2014). Independent optical excitation of distinct neural populations. *Nat. Methods* 11, 338–346.
63. Sweeney, S.T., Broadie, K., Keane, J., Niemann, H., and O'Kane, C.J. (1995). Targeted expression of tetanus toxin light chain in *Drosophila* specifically eliminates synaptic transmission and causes behavioral defects. *Neuron* 14, 341–351.
64. von Philipsborn, A.C., Liu, T., Yu, J.Y., Masser, C., Bidaye, S.S., and Dickson, B.J. (2011). Neuronal control of *Drosophila* courtship song. *Neuron* 69, 509–522.
65. Shirangi, T.R., Stern, D.L., and Truman, J.W. (2013). Motor control of *Drosophila* courtship song. *Cell Rep.* 5, 678–686.
66. Ellis, L.B., and Kessler, S. (1975). Differential posteclosion housing experiences and reproduction in *Drosophila*. *Anim. Behav.* 23, 949–952.
67. Kohatsu, S., and Yamamoto, D. (2015). Visually induced initiation of *Drosophila* innate courtship-like following pursuit is mediated by central excitatory state. *Nat. Commun.* 6, 6457.
68. Riabinina, O., Dai, M., Duke, T., and Albert, J.T. (2011). Active process mediates species-specific tuning of *Drosophila* ears. *Curr. Biol.* 21, 658–664.
69. Fan, P., Manoli, D.S., Ahmed, O.M., Chen, Y., Agarwal, N., Kwong, S., Cai, A.G., Neitz, J., Renslo, A., Baker, B.S., and Shah, N.M. (2013). Genetic and neural mechanisms that inhibit *Drosophila* from mating with other species. *Cell* 154, 89–102.
70. Zhang, S.X., Rogulja, D., and Crickmore, M.A. (2016). Dopaminergic Circuitry Underlying Mating Drive. *Neuron* 91, 168–181.
71. Keleman, K., Vrontou, E., Krüttner, S., Yu, J.Y., Kurtovic-Kozaric, A., and Dickson, B.J. (2012). Dopamine neurons modulate pheromone responses in *Drosophila* courtship learning. *Nature* 489, 145–149.
72. Kamikouchi, A., Inagaki, H.K., Effertz, T., Hendrich, O., Fiala, A., Göpfert, M.C., and Ito, K. (2009). The neural basis of *Drosophila* gravity-sensing and hearing. *Nature* 458, 165–171.
73. Yorozu, S., Wong, A., Fischer, B.J., Dankert, H., Kernan, M.J., Kamikouchi, A., Ito, K., and Anderson, D.J. (2009). Distinct sensory representations of wind and near-field sound in the *Drosophila* brain. *Nature* 458, 201–205.
74. Ishikawa, Y., Okamoto, N., Nakamura, M., Kim, H., and Kamikouchi, A. (2017). Anatomic and Physiologic Heterogeneity of Subgroup-A Auditory Sensory Neurons in Fruit Flies. *Front. Neural Circuits* 11, 46.
75. Patella, P., and Wilson, R.I. (2018). Functional Maps of Mechanosensory Features in the *Drosophila* Brain. *Curr. Biol.* 28, 1189–1203.
76. Azevedo, A.W., and Wilson, R.I. (2017). Active Mechanisms of Vibration Encoding and Frequency Filtering in Central Mechanosensory Neurons. *Neuron* 96, 446–460.

77. Pacheco, D., Thiberge, S., Pnevmatikakis, E., and Murthy, M. (2019). Auditory Activity is Diverse and Widespread Throughout the Central Brain of *Drosophila*. *bioRxiv*. full. <https://doi.org/10.1101/709519v1>.
78. Koganezawa, M., Kimura, K., and Yamamoto, D. (2016). The Neural Circuitry that Functions as a Switch for Courtship versus Aggression in *Drosophila* Males. *Curr. Biol.* 26, 1395–1403.
79. Pan, Y., Meissner, G.W., and Baker, B.S. (2012). Joint control of *Drosophila* male courtship behavior by motion cues and activation of male-specific P1 neurons. *Proc. Natl. Acad. Sci. USA* 109, 10065–10070.
80. Kohatsu, S., Koganezawa, M., and Yamamoto, D. (2011). Female contact activates male-specific interneurons that trigger stereotypic courtship behavior in *Drosophila*. *Neuron* 69, 498–508.
81. Yamada, D., Ishimoto, H., Li, X., Kohashi, T., Ishikawa, Y., and Kamikouchi, A. (2018). GABAergic Local Interneurons Shape Female Fruit Fly Response to Mating Songs. *J. Neurosci.* 38, 4329–4347.
82. Clemens, J., Ozeri-Engelhard, N., and Murthy, M. (2018). Fast intensity adaptation enhances the encoding of sound in *Drosophila*. *Nat. Commun.* 9, 134.
83. Schöneich, S., Kostarakos, K., and Hedwig, B. (2015). An auditory feature detection circuit for sound pattern recognition. *Sci. Adv.* 1, e1500325–e5.
84. Cande, J., Berman, G.J., Namiki, S., Qiu, J., Korff, W., Card, G., et al. (2018). Optogenetic dissection of descending behavioral control in *Drosophila*. *eLife* 7, e34275.
85. Namiki, S., Dickinson, M.H., Wong, A.M., Korff, W., and Card, G.M. (2018). The functional organization of descending sensory-motor pathways in *Drosophila*. *eLife* 7, e34272.
86. Ratcliff, R., Smith, P.L., Brown, S.D., and McKoon, G. (2016). Diffusion Decision Model: Current Issues and History. *Trends Cogn. Sci.* 20, 260–281.
87. Yapici, N., Kim, Y.J., Ribeiro, C., and Dickson, B.J. (2008). A receptor that mediates the post-mating switch in *Drosophila* reproductive behaviour. *Nature* 451, 33–37.
88. Kostarakos, K., Hennig, M.R., and Römer, H. (2009). Two matched filters and the evolution of mating signals in four species of cricket. *Front. Zool.* 6, 22.
89. Capranica, R.R., Frishkopf, L.S., and Nevo, E. (1973). Encoding of geographic dialects in the auditory system of the cricket frog. *Science* 182, 1272–1275.
90. Prather, J.F., Peters, S., Nowicki, S., and Mooney, R. (2008). Precise auditory-vocal mirroring in neurons for learned vocal communication. *Nature* 451, 305–310.
91. Mooney, R. (2014). Auditory-vocal mirroring in songbirds. *Philos. Trans. R. Soc. Lond. B Biol. Sci.* 369, 20130179–20130399.
92. Rizzolatti, G., and Fogassi, L. (2014). The mirror mechanism: recent findings and perspectives. *Philos. Trans. R. Soc. Lond. B Biol. Sci.* 369, 20130420.
93. Rizzolatti, G., and Arbib, M.A. (1998). Language within our grasp. *Trends Neurosci.* 21, 188–194.
94. Hooper, E.D., Jung, Y., Inagaki, H.K., Rubin, G.M., Anderson, D.J., and Ramaswami, M. (2015). P1 interneurons promote a persistent internal state that enhances inter-male aggression in *Drosophila*. *eLife* 4, e11346.
95. Poulet, J.F.A., and Hedwig, B. (2003). Corollary discharge inhibition of ascending auditory neurons in the stridulating cricket. *J. Neurosci.* 23, 4717–4725.
96. Schneider, D.M., Nelson, A., and Mooney, R. (2014). A synaptic and circuit basis for corollary discharge in the auditory cortex. *Nature* 513, 189–194.
97. Chen, T.-W., Wardill, T.J., Sun, Y., Pulver, S.R., Renninger, S.L., Baohan, A., Schreiter, E.R., Kerr, R.A., Oger, M.B., Jayaraman, V., et al. (2013). Ultrasensitive fluorescent proteins for imaging neuronal activity. *Nature* 499, 295–300.
98. Pnevmatikakis, E.A., and Giovannucci, A. (2017). NoRMCorre: An online algorithm for piecewise rigid motion correction of calcium imaging data. *J. Neurosci. Methods* 291, 83–94.
99. Jenett, A., Rubin, G.M., Ngo, T.-T.B., Shepherd, D., Murphy, C., Dionne, H., Pfeiffer, B.D., Cavallaro, A., Hall, D., Jeter, J., et al. (2012). A GAL4-driver line resource for *Drosophila* neurobiology. *Cell Rep.* 2, 991–1001.
100. Rohlfing, T., and Maurer, C.R., Jr. (2003). Nonrigid image registration in shared-memory multiprocessor environments with application to brains, breasts, and bees. *IEEE Trans. Inf. Technol. Biomed.* 7, 16–25.
101. Schindelin, J., Arganda-Carreras, I., Frise, E., Kaynig, V., Longair, M., Pietzsch, T., Preibisch, S., Rueden, C., Saalfeld, S., Schmid, B., et al. (2012). Fiji: an open-source platform for biological-image analysis. *Nat. Methods* 9, 676–682.

STAR★METHODS

KEY RESOURCES TABLE

REAGENT or RESOURCE	SOURCE	IDENTIFIER
Antibodies		
rabbit anti-GFP	Invitrogen	Cat#1828014
mouse anti-Bruchpilot (nc82)	DHSB	Cat#AB2314866
goat anti-rabbit Alexa Flour 488	Invitrogen	Cat#1853312
goat anti-mouse Alexa Flour 633	Invitrogen	Cat#1906490
Chemicals, Peptides, and Recombinant Proteins		
all-trans retinal	Sigma-Aldrich	Cat#R2500
Sigmacote	Sigma-Aldrich	Cat#SL2
S2 insect medium	Sigma Aldrich	Cat#S0146
Experimental Models: Organisms/Strains		
<i>D. melanogaster</i> : NM91, CM07, CarM03, N30, NM91, TZ58, ZH23, ZW109, and Canton S	Canton S is a lab stock; the 8 other strains provided by Peter Andolfatto	N/A
<i>D. melanogaster</i> : Dsx/GCaMP: UAS-20X-GCaMP6m, UAS-tdTomato;dsx-Gal4	dsx-Gal4 provided by Stephan Goodwin UAS-20X-GCaMP6m obtained from the Bloomington <i>Drosophila</i> Stock Center (BDSC). [42, 97]	BDSC Cat#42748 BDSC Cat#36327
<i>D. melanogaster</i> : Dsx/GFP: UAS-2XeGFP; dsx-Gal4	dsx-Gal4 provided by Stephan Goodwin [42]; UAS-2XeGFP from BDSC.	BDSC Cat#6874
<i>D. melanogaster</i> : pC2l/csChrimson: UAS > STOP > CsChrimson.mVenus/8XLexAop2-flp; dsx-LexA, 8xLexAop2-flp/R42B01-Gal4	R42B01-Gal4 and dsx-LexA provided by Bruce Baker; UAS > STOP > CsChrimson.mVenus provided by Vivek Jayaraman; 8xLexAop2-flp obtained from BDSC [27, 43, 62]	BDSC Cat#55820 BDSC Cat#55819
<i>D. melanogaster</i> : pC2l/csChrimson/NM91:UAS > STOP > CsChrimson.mVenus,8XLexAop-flp/NM91; dsx-LexA, 8xLexAop2-flp,R42B01-Gal4/NM91 or UAS > STOP > CsChrimson.mVenus/NM91;dsx-LexA, 8LexAop2-flp,R42B01-Gal4/NM91 or UAS > STOP > CsChrimson.mVenus,8XLexAop-flp/NM91; dsx-LexA, R42B01-Gal4/NM91 (“NM91”)	R42B01-Gal4 and dsx-LexA provided by Bruce Baker; UAS > STOP > CsChrimson.mVenus provided by Vivek Jayaraman; 8xLexAop2-flp obtained from BDSC [27, 43, 62]	BDSC Cat#55819
<i>D. melanogaster</i> : R42B01 ∩ Dsx/GCaMP (pC2l): UAS-20X-GCaMP6m,UAS-tdTomato/+;R42B01-Gal4/+	R42B01-Gal4 provided by Bruce Baker; UAS-20X-GCaMP6m obtained from BDSC [97, 27, 43]	BDSC Cat#42478 BDSC Cat#36327
<i>D. melanogaster</i> : pCd/csChrimson: UAS > STOP > csChrimson/8XLexAop2-flp; dsx-LexA, 8XLexAop2-flp/R41A01-Gal4	UAS > STOP > CsChrimson.mVenus provided by Vivek Jayaraman; R41A01 obtained from BDSC [43, 62]	BDSC Cat#39425 BDSC Cat#55820 BDSC Cat#55819
<i>D. melanogaster</i> : pC2 TNT: UAS > STOP > TNT/8XLexAop-flp; dsx-LexA/R42B01-Gal4	R42B01-Gal4 and dsx-LexA provided by Bruce Baker; UAS > STOP > TNT provided by Barry Dickson [27, 43, 63]	BDSC Cat# 28844
<i>Drosophila melanogaster</i> : pC2 control: +/8XLexAop2-flp; dsx-LexA/R42B01-Gal4	R42B01-Gal4 and dsx-LexA provided by Bruce Baker. [27, 43]	BDSC Cat#55820
<i>Drosophila melanogaster</i> : pC1: R71G01.AD/UAS-myGFP;dsx.DBD/+	R71G01.AD provided by Gerald Rubin, dsx.DBD provided by Stephen Goodwin [79]	BDSC Cat#32198

(Continued on next page)

Continued

REAGENT or RESOURCE	SOURCE	IDENTIFIER
<i>Drosophila melanogaster</i> : pMN2: R57C10-flpG5/+; dsx-Gal4/10UAS > STOP > HA, 10UAS > STOP > V5,10UAS > STOP > FLAG	dsx-Gal4 provided by Stephan Goodwin; rest of the genotype from BDSC [42, 60]	BDSC Cat# 64088
<i>Drosophila melanogaster</i> : pC2: R57C10-flp/+; dsx-Gal4/10UAS > STOP > HA, 10UAS > STOP > V5,10UAS > STOP > FLAG	dsx-Gal4 provided by Stephan Goodwin; rest of the genotype from BDSC [42, 60]	BDSC Cat# 64087
Software and Algorithms		
MATLAB R2017a	Mathworks	https://www.mathworks.com/products/matlab.html
FlySongSegmenter	[30]	https://github.com/murthylab/MurthyLab_FlySongSegmenter
Code for the tracking videos and analyzing FLyTRAP data	This paper	https://github.com/murthylab/FLyTRAP
VFB aligner for image registration		http://vfbaligner.inf.ed.ac.uk/admin
CMTK for image registration	[100]	https://www.nitrc.org/projects/cmtk
FIJI for image processing	[101]	http://fiji.sc

LEAD CONTACT AND MATERIALS AVAILABILITY

This study did not generate new transgenic reagents; transgenic lines used in this study are available upon request. Further information and requests for resources and reagents should be directed to and will be fulfilled by the Lead Contact, Mala Murthy (mmurthy@princeton.edu).

EXPERIMENTAL MODEL AND SUBJECT DETAILS

Drosophila melanogaster flies were raised at low density on a 12:12 dark:light cycle, at 25°C and 60% humidity. Healthy and naive virgin male and female flies were isolated within 6 hours of eclosion and aged for 3–7 days prior to the experiments. Flies were housed in groups of 10–14 individuals of the same sex for the majority of experiments except for the single-housed condition in Figure 6. See Key Resources Table for Information on the genotype of each fly strain used.

METHOD DETAILS**FLyTRAP**

Fly behavior was recorded with PointGrey cameras (FL3-U3-13Y3M-C or FL3-U3-13E4C-C). Grey color frames with a resolution of 1280x960 pixels were acquired at 30 frames per second using custom written software in python and saved as compressed videos. Sound representation was controlled using custom software written in MATLAB. The sound stimuli were converted to an analog voltage signal using a National Instruments DAQ card (PCIe-6343). The signal was then amplified by a Samson s-amp headphone amp and used to drive a speaker (HiVi F6 6-1/2" Bass/Midrange). Sound intensity was calibrated as in [19] by converting the voltage of a calibrated microphone (placed where the fly chambers would be during an experiment) to sound intensity and adjusting the sound amplification to match the target intensity. Sound and video were synchronized by placing into the camera's field-of-view a 650nm LED whose brightness was controlled using a copy of the sound signal. The chamber consisted of an array of 12 small arenas (7 by 46 mm, made from red plastic) was placed in front of the loudspeaker (Video S1). The arena floor consisted of plastic mesh to let sound into the chamber and the top was covered with a thin, translucent plastic sheet. Flies were illuminated using a white LED back light from below and a desk lamp from above.

Playback experiments

Flies were introduced gently into the chamber using an aspirator. Recordings were performed at 25°C and timed to start within 60 minutes of the incubator lights switching on to catch the morning activity peak. Stimulus playback was block-randomized to ensure that all stimuli within a set occur at the same overall rate throughout the stimulus. The stimulus set (e.g., five pulse trains with different IPIs) was repeated for the duration of the experiment (2 hours). See Table S1 for a list of all stimulus sets. Stimuli were interleaved by 60 s of silence to reduce crosstalk between responses to subsequent stimulus presentations.

Stimulus design

Sound was generated at a sampling frequency of 10 kHz using custom MATLAB scripts. Sine song stimuli were created as pure tones of the specified frequency and intensity (typically 5mm/s). Pulse song was generated by arranging Gabor wavelets in trains interleaved by a specified pause. The Gabor wavelets were built by modulating the amplitude of a short sinusoidal using a Gaussian: $\exp(-t^2/(2\sigma^2)) \sin(2\pi f * t + \phi)$, where f is the pulse carrier frequency, ϕ is the phase of carrier, and σ is proportional to the pulse duration. See [Table S1](#) for the parameters for all stimuli used along with the behavioral responses obtained in FLyTRAP.

Analysis of FLyTRAP data

Fly positions were tracked using custom-written software. Briefly, the image background was estimated as the median of 500 frames spaced to cover the full video. Foreground pixels (corresponding to the fly body) were identified by thresholding the absolute values of the difference between each frame and the background estimate. The fly center position was then taken as the median of the position of all foreground pixels in each chamber. The sequence of fly positions across video frames was then converted into a time series using the light onset frames of the synchronization LED (indicating sound onset) as a reference. From the position time series fly speed was calculated and the speed traces were then aligned to stimulus onset for each trial. Base line speed was calculated as the average of the speed over an interval starting 30 s and ending 2 s before stimulus onset. Test speed was calculated over an interval starting at stimulus onset and ending 2 s after stimulus offset. Tuning curves were calculated as the difference between baseline speed and test speed for each trial, averaged over trials for each stimulus and animal. Speed traces were obtained by subtracting the baseline speed from the trace for each trial and averaging over trials for each stimulus and animal. All data (tuning curves, speed traces) are presented as mean \pm SEM over flies. Code for stimulus generation, fly tracking and analysis of the locomotion data is available at <https://github.com/murthylab/FLyTRAP>.

Manual scoring of wing extension in FLyTRAP

To evaluate the number of flies that extend their wings upon playback of pulse or sine song, we manually scored wing extension in the videos using the VirtualDub software. For pulse song (see [Video S2](#)), we scored 25 stimuli/fly, choosing trials randomly but ensuring that each IPI (16/36/56/76/96 ms) was scored 5 times/fly. To avoid bias, the scorer was blind to the IPI presented to the fly in each trial. A total of 120 male flies and 36 female flies were scored (3000 and 900 single-fly responses total for pulse song). We scored wing extension only when the wing was extended in the first 1/3 s following stimulus onset, and only when the wings were not extended during the 1 s before stimulus onset. For sine song (150Hz carrier frequency), 60 males were scored.

Joint tuning for pulse duration and pause

To visualize locomotor ([Figures S2E](#) and [S2F](#)) and calcium ([Figures S3A](#) and [S3B](#)) responses to pulse trains with different combinations of pulse duration and pulse pause we generated smooth surface plots using MATLAB's "scatteredInterpolant" function with the interpolation mode set to "natural." The boundaries of the plots were set as follows: Pulse duration of zero corresponds to silence and the speed values were set to 0 since all speed traces are always base line subtracted. A pulse pause of zero corresponds to a continuous oscillation and we set the corresponding speed values to those obtained for a 4 s pure tone with a frequency of 250 Hz.

Measurement of song features from song

The inter-pulse interval (IPI) is given by the interval between the peaks of subsequent pulses in a pulse train. Pulse trains correspond to continuous sequences of pulses with IPIs smaller than 200ms. Measuring the pulse durations from natural song data is non-trivial since pulses vary in their shape and can be embedded in background noise. We quantified pulse duration by 1) calculating the envelope of each pulse using the Hilbert transform, 2) smoothing that envelope using a Gaussian window with a standard deviation of 2 ms, and 3) taking as the pulse duration the full width of the smoothed envelope at 20% of the maximum amplitude of the pulse. Pulse durations for artificial stimuli used in our pulse train were defined to be consistent with this method. Pulse carrier frequency is given by the center of mass of the amplitude spectrum of each pulse [[17](#)]. Sine carrier frequency was calculated as the peak frequency of the power spectrum of individual sine tones.

PCA of speed traces

For the PCA of sex-specific responses to sound and optogenetic activation of pC2 ([Figures 5I](#) and [5L](#)) we collected male and female speed traces for all IPIs and optogenetic activation levels into a large matrix. Each speed trace was cut to include only the 10 s after sound onset and then normalized to have zero mean and unit variance.

Optogenetic experiments

CsChrimson was expressed in pC2 neurons using an intersection between R42B01-Gal4 and dsx-LexA using two different genotypes (see table, pC2/csChrimson and pC2/csChrimson/NM91). 655nm light was emitted from a ring of 6 Tri-Star LEDs (LuxeonStar, SinkPAD-II 20mm Tri-Star Base) in FLyTRAP. Flies were fed with food that contained all-trans retinal for a minimum of three days post eclosion. Control flies were raised on regular fly food after eclosion. LED stimulation lasted four seconds with 60 s pause between stimuli, similar to the temporal pattern used for auditory stimulus delivery in FLyTRAP (1-5 mW/cm², 100 Hz, duty cycle 0.5). Smaller intensities of 0.1-1 mW/cm² were not sufficient to drive changes in speed in the pC2/csChrimson/NM91 genotype (data not shown). To measure the amount of song driven by pC2 activation in solitary flies of the pC2/csChrimson and the pC2/csChrimson/NM91

genotype, we used a chamber whose floor was tiled with 16 microphones to allow recording of the song (Figure 5A; Video S5; see [17]). The LED (627nm LEDs, LuxeonStar) was on for four seconds (frequency 25 Hz, duty cycle 0.5) and off for 60 s. For pC2/csChrimson, we tested three different light intensities (1.8, 9, and 13 mW/cm²) that were presented in 3 blocks of 18 trials. The order of the three blocks (light intensities) was randomized for each fly. pC2/csChrimson/NM91 was tested with 9 mW/cm² in 10 trials. Fly song was segmented as described previously [15, 30].

PC2 inactivation during courtship

Tetanus neurotoxin light chain (TNT) [63] was used to block synaptic transmission in pC2 neurons in females and males. 3-7 days old virgin females or males (pC2-TNT: UAS > STOP > TNT/LexAop-flp; dsx-LexA/R42B01-Gal4, pC2-control: +/LexAop-flp; dsx-LexA/R42B01-Gal4) were paired with wild-type flies (NM91) of the opposite sex, in a custom-built chamber designed to record fly song (:25 mm diameter, tiled with 16 microphones; same setup as the one used for measuring optogenetic driven song). Flies were allowed to interact for 30 minutes, and the percent of flies copulated as a function of time was scored. A monochrome camera (Point Grey, FL3-U3-13Y3M) was used to record the fly behavior at 60 frames per second. Fly position was tracked offline and song was segmented as previously described [15, 30]. We then calculated song statistics (e.g., amount of song or number of pulses per window) and female locomotion (average female speed) in windows of 60 s with 30 s overlap [19]. For the rank correlations between male song features and female speed (Figures 5M–5O), we binned the female speed values into 16 bins with the bin edges chosen such that each bin was populated by an equal amount of samples (see Figure 5M) and calculated the rank correlation between the binned female speed and the average male song feature per bin. Changes in correlation between control and experimental flies (Figure 5O) were analyzed using an ANCOVA model with independent slopes and intercepts. Significance was determined based on the p value of the interaction term (model's genotype by song-feature) after Bonferroni correction.

Calcium imaging

Imaging experiments were performed on a custom built two-photon laser scanning microscope equipped with 5mm galvanometer mirrors (Cambridge Technology), an electro-optic modulator (M350-80LA-02 KD*P, Conoptics) to control the laser intensity, a piezo-electric focusing device (P-725, Physik Instrumente) for volumetric imaging, a Chameleon Ultra II Ti:Sapphire laser (Coherent) and a water immersion objective (Olympus XLPlan 25X, NA = 1.05). The fluorescence signal collected by the objective was reflected by a dichroic mirror (FF685 Dio2, Semrock), filtered using a multiphoton short-pass emission filter (FF01-680/sp-25, Semrock), split by a dichroic mirror (FF555 Dio3, Semrock) into two channels, green (FF02-525/40-25, Semrock) and red (FF01-593/40-25, Semrock), and detected by GaAsP photo-multiplier tubes (H10770PA-40, Hamamatsu). Laser power (measured at the sample plane) was restricted to 15 mW. The microscope was controlled in MATLAB using ScanImage 5.1 (Vidrio). Single plane calcium signals (Figures 3C–3I, 4F, 4G, and pMN2 neuron in Figures 4C and 4D) were scanned at 8.5 Hz (256X256 pixels). Pixel size was ~0.5 μmX0.5 μm when imaging the LJ or pC2I process and ~0.25 μmX0.25 μm when imaging cell bodies in a single plane (Figures 4G and 4H and pMN2 in Figures 4C and 4D). For volumetric scanning of cell bodies (Figures 4C, 4D, and S4A), volumes were acquired at 0.5Hz (256*216, 20 planes, voxel size ~0.34 μm X 0.4 μm X 1.5 μm), scanning one group of cells at a time (pC1, pC2, pCd).

After surgery (opening of the head capsule to reveal the brain), flies were placed beneath the objective and perfusion saline was continuously delivered directly to the meniscus. Sound playback was controlled using custom written MATLAB software [82]. The software also stopped and started the calcium imaging via a TTL pulse sent to ScanImage (“external hardware trigger” mode), and single frames were synchronized with stimulus by sensing a copy of the Y-galvo mirror to a National Instruments DAQ card (PCIe-6343) that controlled the stimulus. The sound stimulus was generated at a sampling rate of 10kHz and sent by the DAQ card through an amplifier (Crown, D-75A) to a set of head phones (Koss, ‘The Plug’). A single ear plug was connected to one side of a plastic tube (outer-inner diameters 1/8”-1/16”) and the outer tube tip was positioned 2 mm away from the fly arista. Sound intensity was calibrated by measuring the sound intensity 2 mm away from the tube tip with a pre-calibrated microphone at a range of frequencies (100Hz-800Hz) and the output signal was corrected according to the measured intensities. The pause between stimulus representation was 25 s. A stimulus set (26-36 stimuli) was presented to each fly in a block-randomized order as in the playback experiments. Three blocks were presented for each fly. If the response decayed in the middle of a block (possibly because of drift in the z axis), the whole block was discarded from the analysis. Typically, two full repetitions per fly were used for analysis.

Regions of interest (ROIs) for calcium response measurements (in the LJ, pC2 process and in single Dsx+ somata) were selected manually based on a z-projection of the tdTomato channel. ΔF/F of the GCaMP signal was calculated as $(F(t)-F_0)/F_0$, where F_0 is the mean fluorescence in the ROI in the 10 s preceding stimulus onset. Integral ΔF/F (Figures 3D and 3F–3I) and peak ΔF/F (Figures S3F and S3G) values were calculated in a window starting at sound stimulus onset and ending 25 s after sound stimulus offset. To compensate for differences in overall responsiveness across flies, we normalized ΔF/F values of each fly by dividing the integral or peak ΔF/F by the maximal value (of integral or peak ΔF/F) across all stimuli for that fly. For volumetric scanning (Figures 4C, 4D, and S4A) pulse song (250Hz, 16 pulse duration, 20 pulse pause), sine song (250 Hz) and broadband noise (100-900Hz) were presented 6 times each (in the order pulse-sine-noise, 6 blocks, duration of each stimulus 10 s with 20 of silence in between) for each group of neurons (pC1 or pC2). A cell was considered responsive to a given stimulus (pulse, sine or broadband noise) if the mean ΔF during the stimulus was higher than the mean ΔF in the 10 s before stimulus onset in 5/6 blocks. Each time series was first motion corrected using the rigid motion correction algorithm NorMCorre [98] taking the tdTomato signal as the reference image. Then, single cell bodies were drawn manually, by marking cell boundaries stack by stack. In some cases, mostly with male pC1

neurons, cell bodies were very packed, such that some ROIs we marked manually possibly included more than a single cell. The number of single cells reported from Ca imaging is therefore slightly underestimated.

Light microscopy

Flies expressing GFP in Dsx+ neurons (UAS-eGFP2X; dsx-Gal4; [Figure 3A](#)) and flies expressing CsChrimson.mVenus in pC2 neurons (R42B01-Gal4 intersected with dsx-LexA; [Figure S5A](#)) were immunostained and scanned in a confocal microscope. 2-4 day old flies were cold-anesthetized on ice, dissected in cold S2 insect medium (Sigma Aldrich, #S0146) and fixed for 30-40 minutes on a rotator at room temperature in 4% PFA in 0.3% PBTS (0.3% Triton in PBS), followed by 4x15 minutes washes in 0.3% PBTS and 30 minutes in blocking solution (5% normal goat serum in 0.3%PBTS). Brains were incubated over two nights at 4°C with primary antibody, washed with 0.3%PBT and incubated for two more nights at 4°C in secondary antibody, followed by washing (4x15 minutes in 0.3%PBTS and 4x20 minutes in PBS), and mounting with Vectashield for 2-7 days before imaging. Antibodies were diluted in blocking solution at the following concentrations: rabbit anti-GFP (Invitrogen #1828014; used against GFP and mVenus) 1:1000, mouse anti-Bruchpilot (nc82, DSHB AB2314866) 1:20, goat anti-rabbit Alexa Flour 488 (Invitrogen #1853312) 1:200, goat anti-mouse Alexa Flour 633 (Invitrogen #1906490) 1:200.

Stochastic labeling of Dsx+ neurons in the female brain ([Figures 4A](#) and [4E](#)) was done using multi-color-flip-out (MCFO, [60]) with three different epitope tags (HA,V5,FLAG). We followed the JFRC FlyLight Protocol ‘IHC-MCFO’ (<https://www.janelia.org/project-team/flylight/protocols>) for the preparation of brains. Flp was induced using R5710C10 promotor-coding sequence fusions of the flpG5 and flpI. Flies were 4-7 days old when dissected. Flies were stored at 25°C. Confocal stacks were acquired with a white light laser confocal microscope (Leica TCS SP8 X) and a Leica objective (HC PL APO 20x/0.75 CS2). A high-resolution scan of a pC2 cell ([Figure 4E](#)) was performed with an oil immersion Leica objective (HC PL APO 63x/1.40 Oil CS2, [Figure 4E](#)). Images were registered to the Janelia brain template (JFRC2) [99] using vfaligner (<http://vfaligner.inf.ed.ac.uk/admin>), which internally uses CMTK for registration [100]. The images of the fly brain in [Figures 4A](#) and [S4D](#) were deposited by G. Jefferis [56, 57]. Image processing was performed in FIJI [101].

QUANTIFICATION AND STATISTICAL ANALYSIS

All statistical analyses were performed in MATLAB. Since the majority of our data did not follow normal distributions as determined by Jarque-Bera tests we used non-parametric tests throughout. Association tests were based on used Spearman’s rank correlation ([Figures 2, 3, 4, and 5](#)). Measures of central tendency were compared using two-sided Wilcoxon rank sum tests ([Figures 3C and 6C](#)). Proportions were compared using a Chi-square test ([Figure 2F](#)). Details on each statistical analysis including exact values of n, what n represents, definition of center and dispersion can be found in the figure legends and in Results.

DATA AND CODE AVAILABILITY

Code for tracking videos and analyzing behavioral responses in FLyTRAP is available at <https://github.com/murthylab/FLyTRAP>. The published article includes behavioral and neuronal data generated or analyzed during this study in [Table S1](#). Raw data supporting the current study have not been deposited in a public repository because of their large size, but are available from the Lead Contact, Mala Murthy (mmurthy@princeton.edu) upon request. Pictograms of flies were modified from Benjamin de Bivort’s lab web page.